

Deepak KUMAR

Vineet Gautam

 SCI Paper

Document Details

Submission ID

trn:oid:::27535:142329914

Submission Date

Jun 9, 2026, 10:17 PM GMT+5:30

Download Date

Jun 9, 2026, 10:20 PM GMT+5:30

File Name

CHAPTER 1.docx

File Size

5.8 MB

49 Pages

9,841 Words

56,772 Characters





7% Overall Similarity

The combined total of all matches, including overlapping sources, for each database.




Filtered from the Report

- ▶ Bibliography
- ▶ Quoted Text
- ▶ Cited Text
- ▶ Small Matches (less than 12 words)

Match Groups

-  **33 Not Cited or Quoted 7%**
Matches with neither in-text citation nor quotation marks
-  **0 Missing Quotations 0%**
Matches that are still very similar to source material
-  **0 Missing Citation 0%**
Matches that have quotation marks, but no in-text citation
-  **0 Cited and Quoted 0%**
Matches with in-text citation present, but no quotation marks

Top Sources

- 4%  Internet sources
- 2%  Publications
- 6%  Submitted works (Student Papers)

Match Groups

- **33 Not Cited or Quoted 7%**
Matches with neither in-text citation nor quotation marks
- **0 Missing Quotations 0%**
Matches that are still very similar to source material
- **0 Missing Citation 0%**
Matches that have quotation marks, but no in-text citation
- **0 Cited and Quoted 0%**
Matches with in-text citation present, but no quotation marks

Top Sources

- 4% Internet sources
- 2% Publications
- 6% Submitted works (Student Papers)

Top Sources

The sources with the highest number of matches within the submission. Overlapping sources will not be displayed.

1	Student papers	Napier University on 2023-08-28	1%
2	Student papers	University of Derby on 2026-01-15	<1%
3	Student papers	The University of Manchester on 2026-05-05	<1%
4	Internet	ijcrt.org	<1%
5	Student papers	University of Greenwich on 2026-03-24	<1%
6	Internet	www.researchgate.net	<1%
7	Student papers	Edith Cowan University on 2026-06-05	<1%
8	Publication	Md Ehtesham, Majid Jamil. "Control techniques for enhancing performance of PV ..."	<1%
9	Student papers	Universiti Malaysia Perlis on 2026-01-02	<1%
10	Publication	Soro, Sielle Martin. "Etude, Simulation et Controle d'un Systeme D'energies Reno..."	<1%

11	Student papers	University of Hertfordshire on 2022-04-29	<1%
12	Student papers	University of Teesside on 2024-04-26	<1%
13	Publication	Youssef Achour, Asmae El Mokrini, Rachid El Mrabet, Asmae Berrada. "Optimizing..."	<1%
14	Internet	pub.epsilon.slu.se	<1%
15	Internet	wiredwhite.com	<1%
16	Student papers	Curtin University of Technology on 2020-11-09	<1%
17	Student papers	Higher Education Commission Pakistan on 2022-05-23	<1%
18	Publication	Kim, Yong Sin, Sung-Mo Kang, Bruce Johnston, and Roland Winston. "A novel met..."	<1%
19	Student papers	Queen Mary and Westfield College on 2026-05-13	<1%
20	Student papers	University of Newcastle upon Tyne on 2016-03-10	<1%
21	Internet	www.iitbbs.ac.in	<1%
22	Student papers	University of Derby on 2025-05-11	<1%
23	Publication	Zheng Wang, Shouting Fan, Yang Zheng, Ming Cheng. "Control of a six-switch in..."	<1%
24	Internet	dokumen.pub	<1%

25	Internet	ntnuopen.ntnu.no	<1%
26	Publication	Subhendu Sekhar Sahoo, Govind Singh Jethi, Debasish Mishra, K. Suryanarayana ...	<1%
27	Internet	aast.edu	<1%
28	Internet	ir.uitm.edu.my	<1%
29	Internet	open.library.ubc.ca	<1%
30	Internet	www.mdpi.com	<1%

CHAPTER 1

INTRODUCTION

1.1 INTRODUCTION

The shift from traditional fossil fuel-based power generation to renewable energy technologies has accelerated due to the growing demand for clean, sustainable, and ecologically responsible energy sources worldwide. Solar photovoltaic (PV) systems have drawn a lot of interest among the several renewable energy sources (RES) because of their widespread availability, modular design, little maintenance needs, and steadily declining installation costs. One of the most appealing ways to lessen carbon footprints and solve the world's energy problems is solar PV technology, which directly transforms solar energy into electrical energy without emitting any harmful emissions [1]. The efficiency and dependability of PV systems have been significantly enhanced in recent years by quick developments in semiconductor technology, power electronic converters, and intelligent control methods, which have encouraged their broad use in commercial, industrial, and residential settings [2]. In order to accomplish long-term energy security and sustainable development objectives, governments and energy organizations around the world are also aggressively encouraging the deployment of solar energy through supportive policies and incentives.

Despite these benefits, the output power produced by solar panels is largely reliant on environmental factors, including temperature, cloud cover, sun irradiance, and weather fluctuations, which present some operational issues for solar PV systems [3]. Solar energy is irregular and sporadic nature, causing variations in voltage and power production, which can have a detrimental impact on the power system's stability and dependability. PV generation drastically drops during cloudy or nighttime hours, which results in insufficient power supply for linked loads or the utility grid [4]. Specifically in

standalone and weak-grid applications, these fluctuations make it challenging to maintain steady power delivery, voltage management, and frequency stability. Additionally, abrupt variations in solar radiation can cause power-quality problems such as voltage swings, harmonics, and instability in converter systems' DC-link voltage. For solar-based power systems to operate continuously and dependably, effective energy management and sophisticated control techniques are crucial [5].

In order to get around these restrictions, integrating battery energy storage systems (BESS) with solar PV power has proven to be a dependable and efficient way to improve system performance, energy management, and grid stability [6]. In order to provide continuous power availability and minimize variations in PV output, the BESS stores extra energy produced during peak sunshine hours and supplies electricity during times of low solar generation or increasing load demand. Improved power quality, better voltage and frequency management, less energy waste, and better use of renewable energy resources are only a few benefits of the combined PV-BESS system. Advanced power electronic converters, bidirectional DC-DC converters, synchronized inverter management approaches, and Maximum Power Point Tracking (MPPT) methods are used in contemporary grid-connected applications to achieve stable system operation and effective energy transmission [7]. Effective DC-link voltage management, efficient battery charging and discharging, and smooth integration with the utility grid are all made possible by proper coordination between the PV array, battery storage unit, and inverter control system [8]. As a result, the PV-BESS integrated system offers a dependable, adaptable, and effective way to satisfy future energy needs while encouraging the production of sustainable and green power [9].

1.2 BACKGROUND AND MOTIVATION

With growing environmental concerns, increased electricity demand, and the need to lessen reliance on fossil fuels, global energy systems are quickly moving toward RES. Because of their clean functioning, modular design, and declining installation prices, solar PV systems have emerged as one of the most popular renewable technologies [10]. To satisfy future energy needs, large-scale PV system implementation is being promoted in nations like India. However, PV systems' output power is sporadic and unpredictable

due to its strong dependence on temperature and solar irradiance. Weather variations can result in voltage and power output fluctuations, which can cause instability and inconsistent power supply to the associated load [11].

Integrating a BESS with the PV system has shown to be a successful way to increase system dependability and guarantee a steady power supply [12]. The primary goal of the PV-BESS integrated system is to provide steady, continuous power to the load in a variety of load and environmental circumstances. By storing extra energy during times of strong PV generation and supplying electricity during times of low generation, the battery lowers power fluctuations and enhances system performance [13]. Furthermore, power electronic converters and sophisticated control algorithms support energy management, power quality, and DC-link voltage stability. As a result, the PV-BESS system offers a dependable and effective method for steady power distribution based on renewable energy [14].

1.3 NEED FOR GRID-INTEGRATED PV-BESS SYSTEM

As solar energy is intermittent, the increasing utilization of solar PV systems in contemporary power networks has created several operational issues. When solar irradiation and load demand fluctuate, conventional grid-connected PV systems lacking energy storage cannot supply the load with steady, continuous electricity [15]. Due to this, it becomes challenging to maintain power balance, voltage stability, and dependable performance under dynamic operating situations. Therefore, to enhance system performance and guarantee continuous power delivery, a BESS must be integrated with PV generation [16].

1.3.1 Stable power supply to the load

Managing steady and continuous power delivery to the associated load is the essential prerequisite for a grid-integrated PV-BESS system. The generated power may not always match the load demand because PV output changes with weather and sun irradiance [17]. To maintain power balance and ensure reliable operation, the BESS stores excess energy

during periods of high PV generation and provides electricity during periods of low generation.

1.3.2 Enhanced reliability and energy management

Improved operational reliability during abrupt load fluctuations, grid disruptions, and transient faults is provided by a PV system coupled with BESS [18]. By balancing generation and demand, the battery storage system serves as an energy buffer and facilitates efficient energy management [19]. This makes it possible to use renewable energy supplies more effectively and improves the power system's overall flexibility and efficiency.

1.4 ROLE OF BATTERY ENERGY STORAGE (BESS)

The integration of BESS provides multiple technical and operational benefits:

1.4.1 System stability improvement

The BESS helps to maintain a constant DC-link voltage and reduces power fluctuations caused by variations in solar PV production. It improves overall system stability by offering quick dynamic reaction to abrupt changes in solar irradiation and load demand [20]. Additionally, by regulating the disparity between power generation and load need, the battery storage system enables consistent and dependable power delivery.

1.4.2 Load management and peak shaving

In order to ensure a balanced power supply to the load, a surplus of energy produced during low-load situations is stored in the battery and used during peak demand periods. This procedure increases overall energy use efficiency and lessens the strain on the power system. Additionally, it aids in sustaining steady and continuous power supply in the face of abrupt spikes in load demand.

1.4.3 Backup support and renewable energy integration

The BESS allows for higher integration of renewable energy into the power system and ensures that key loads have an uninterrupted power supply during grid disruptions or low PV generation [21].

1.5 SYSTEM OVERVIEW

A PV producing unit, DC–DC boost converter, DC-link, battery energy storage system, Voltage Source Inverter (VSI), and sophisticated control system make up the proposed grid-connected PV system backed by the BESS [22]. While the boost converter raises the PV output voltage and executes MPPT operation for effective power extraction, the PV array transforms solar energy into DC electrical power [23]. To maintain steady DC-link voltage and guarantee seamless power transmission throughout the system, a DC-link capacitor is used. Furthermore, regulated charging and discharging operations based on solar output and load demand circumstances are supported by the BESS.

In order to serve the linked load and interface with the utility grid, the grid-connected inverter system transforms the DC-link power into synchronized AC power [24]. To provide steady and dependable power transmission, the inverter maintains appropriate voltage, frequency, and phase synchronization. Additionally, sophisticated control methods including MPPT control, DC-link voltage regulation, battery State of Charge (SOC) management, PLL synchronization, and dq-axis current control, are used to regulate the entire functioning of the proposed PV–BESS integrated system. Under various load and environmental situations, these coordinated control solutions enhance energy management, system stability, and continuous power delivery [25].

1.6 CHALLENGES IN PV–BESS INTEGRATION

The stability and dependability of the entire system are influenced by a number of operational and technological difficulties that occur when PV systems are integrated with BESS. Solar energy is intermittent and unpredictable because the PV array's output power is heavily influenced by temperature, weather, and solar irradiation [26]. It is challenging to maintain a steady DC-link voltage and continuous power supply to the load because of these ongoing variations in PV generation, which cause fluctuations in

voltage and power output. Rapid variations in solar power also make converter control more complex and require a quick dynamic response to guarantee steady and seamless system operation in a range of environmental circumstances [27].

Coordinating and managing the grid-connected inverter and battery storage system effectively is another significant problem. To increase battery life and efficiency, the BESS must manage repeated cycles of charging and discharging while operating within safe State of Charge (SOC) restrictions [28]. While reducing switching losses, the bidirectional converter attached to the battery should react to abrupt changes in load and variations in PV output. To achieve good power quality and dependable grid operation, it is also crucial to maintain grid synchronization, regulate active and reactive power flow, and minimize harmonics and voltage variations. Therefore, reliable and effective PV-BESS system integration requires effective control strategies and coordinated energy management methodologies [29].

1.7 OBJECTIVE OF THE DISSERTATION

This dissertation's main goal is to design and evaluate a three-phase grid-connected PV system with battery energy storage assistance that can supply a connected load with steady, dependable, and effective power under a variety of operating and environmental circumstances. The main system components, such as the PV array, DC–DC boost converter, BESS, bidirectional converter, DC-link, and grid-connected inverter, are the focus of the study [30]. In spite of variations in solar irradiation, temperature, and load demand, special attention is paid to sustaining continuous power flow and enhancing overall system stability.

Implementing efficient control algorithms for optimal system performance and good energy management is another key goal of this effort. This involves using battery management control for safe charging and discharging, DC-link voltage regulation for steady converter performance, and MPPT techniques to harvest the maximum amount of solar power that is available. Using inverter control strategies including Phase-Locked Loop (PLL) and dq-axis current management, the dissertation also seeks to improve power quality and ensure optimal grid synchronization [31]. Additionally, modeling

studies that take into account factors like voltage stability, power quality, harmonic performance, inverter response, battery dynamics, and dependability of power supply to the load are used to assess the overall performance of the PV–BESS integrated system. The final goal of the planned effort is to show how well PV–BESS integration works for reliable and effective renewable energy-based power systems [32].

1.8 SCOPE OF THE WORK

9 The modeling, control, and performance analysis of a three-phase grid-connected photovoltaic (PV) system backed by a battery energy storage system (BESS) are the main topics of this dissertation. Using the MATLAB/Simulink environment, the PV array, DC–DC boost converter, battery energy storage system, bidirectional converter, DC-link, and grid-connected Voltage Source Inverter (VSI) are all thoroughly modeled. To guarantee steady and dependable system functioning, sophisticated control strategies such Maximum Power Point Tracking (MPPT), battery charge-discharge management, DC-link voltage regulation, dq-axis inverter control, and Phase-Locked Loop (PLL) synchronization are used. In order to assess voltage stability, power flow management, battery performance, and continuous power supply capabilities, the suggested system is tested under various solar irradiance and load situations.

28 The thesis is organized into five major sections. The introduction, background, motivation, goals, scope of work, and difficulties related to the integration of photovoltaic (PV) systems and battery energy storage systems (BESS) are presented in the first part. The modeling and system design of the main parts of the suggested PV–BESS integrated system, such as the PV array, converters, battery system, inverter, and grid interface, are described in the second section. The control algorithms used for MPPT, battery management, DC-link voltage regulation, and grid synchronization are covered in the third part. The simulation results and a thorough performance analysis of the system under various operating situations are presented in the fourth part. The last part provides a summary of the dissertation's general conclusions, major contributions, limits, future scope, and closing thoughts.

CHAPTER 2

SYSTEM MODELLING

2.1 INTRODUCTION

Analyzing the behavior and performance of a three-phase grid-connected PV system supplemented by battery energy storage requires system modeling. Understanding system dynamics and creating efficient control strategies requires accurate modeling of the main system components, including the PV array, DC–DC converters, BESS, inverter, filter, and grid interface shows in Fig. 2.1. Evaluating system stability, power flow, voltage regulation, and overall operational performance under various environmental and load situations is made easier with the correct mathematical representation of these components.

The proposed PV–BESS integrated system's comprehensive modeling and overall system configuration are presented in this chapter. The created models are used to examine how various subsystems interact and to research how the system functions as solar irradiance, load demand, and grid circumstances vary. In order to guarantee steady and dependable power delivery to the load, the modeling approach also facilitates the use of control strategies for MPPT, battery energy management, DC-link voltage regulation, and grid synchronization.

The coordinated operation of the PV array, utility grid, power converters, inverter, and BESS is represented by the overall system model. The MPPT-controlled boost converter guarantees maximal power extraction and constant DC-link voltage when the PV system produces DC power. By storing extra electricity and providing energy when PV generation is low, the BESS promotes energy balancing. In order to serve the load and

interface with the grid, synchronized AC power with stable operation is provided via the inverter and LC filter.

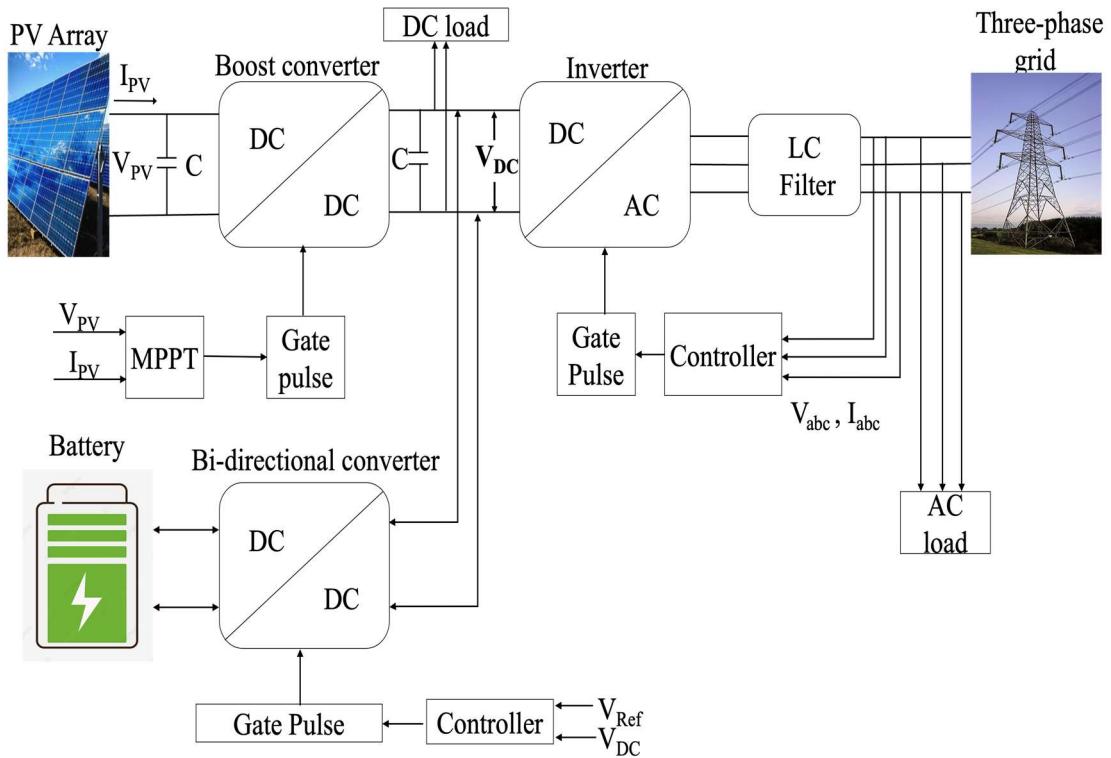


Fig. 2.1. Schematic representation of a dual-stage converter with BESS.

2.2 PHOTOVOLTAIC (PV) ARRAY MODELLING

A PV cell is a semiconductor device that uses the PV effect to directly convert solar energy into electrical energy. The mobility of charge carriers within the semiconductor material causes the PV cell to produce electrical energy when sunlight strikes it. Environmental factors like temperature and sun irradiation have a significant impact on a PV cell's performance. While a greater temperature lowers the output voltage and overall efficiency of the PV system, an increase in solar irradiation increases the output current and generated power. Because PV features are nonlinear, precise modeling of the PV array is necessary for evaluating system performance and creating efficient control techniques.

PV module or array that can supply the necessary voltage and current levels is created by connecting several PV cells in parallel and series. Table 1 represents the PV array parameters. The single-diode equivalent circuit model is frequently used to describe the

PV array for simulation and analysis purposes. Series resistance (R_s), shunt resistance (R_{sh}), a diode, and a photocurrent source make up this model. The current produced by solar radiation is represented by the photocurrent source, and internal recombination losses are represented by the diode. Internal conduction and leakage losses in the PV cell are taken into consideration by the series and shunt resistances. The created PV model facilitates the application of MPPT techniques for effective power extraction and aids in the investigation of the system's electrical behavior under various operating situations.

TABLE 2.1. PV Array parameters

Parameters	Value
Parallel strings	2
Series strings	15
Maximum Power	250.20 W
V_{oc}	37.30 V
I_{sc}	8.66 A
V_{mpp}	30.70 V
I_{mpp}	8.15 A
Total power	7500 W

The current-voltage (I-V) and power-voltage (P-V) characteristics of the PV array under various sun irradiation circumstances are displayed in Fig. 2.2. The I-V characteristics are seen in the upper graph, where the output current first stays almost constant before rapidly declining close to the open-circuit voltage region. The P-V characteristics are depicted in the lower graph, which demonstrates how the output power rises with voltage and approaches the Maximum Power Point (MPP). It is noticeable that while the output voltage barely changes, a rise in solar irradiance dramatically raises the output current and maximum power produced by the PV array. These features show the PV system nonlinear behavior and emphasize the significance of MPPT methods for obtaining the most power possible in a range of environmental circumstances. The graphs show that the MPP varies with variations in solar irradiation, necessitating ongoing monitoring for effective system performance. Under order to maintain optimum PV performance, increase energy harvesting efficiency, and guarantee reliable power supply under dynamic environmental circumstances, MPPT approaches are crucial.

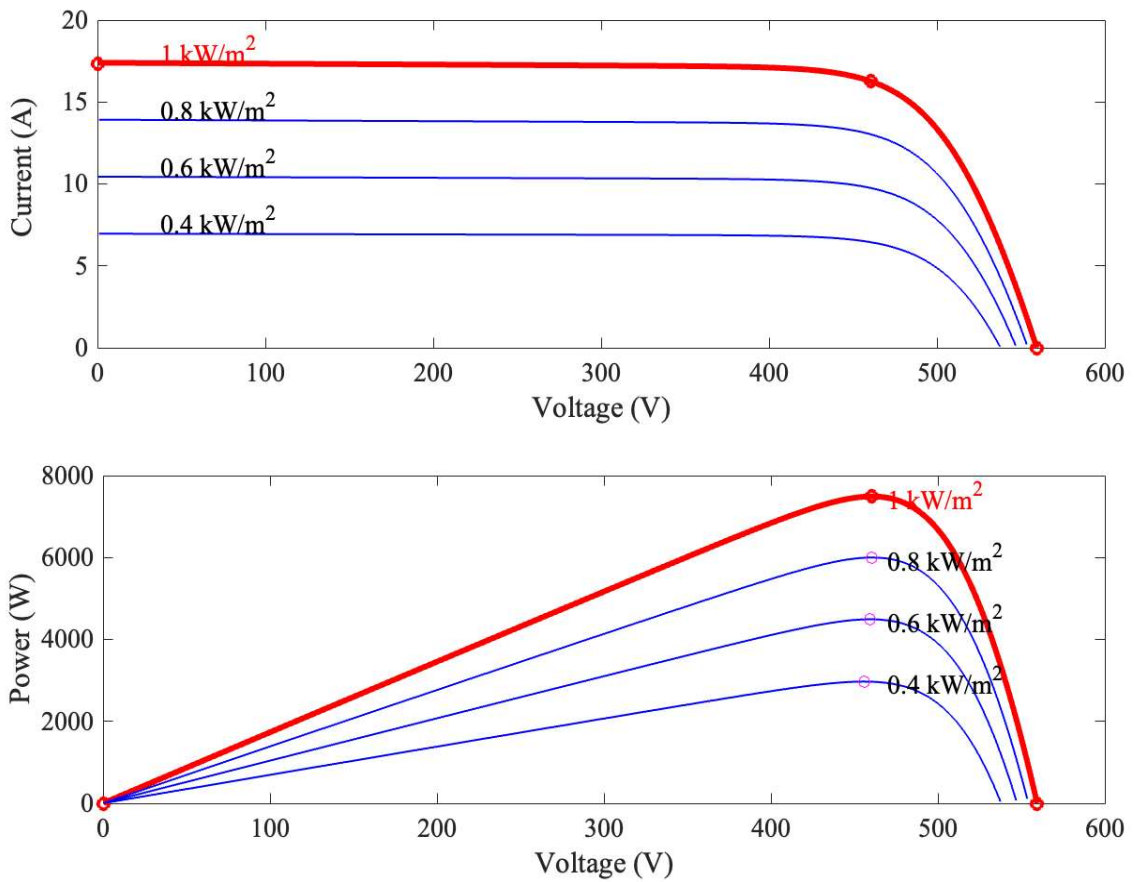


Fig. 2.2 Characteristic curve of PV

2.2.1 Single-diode model derivation

$$I = I_{ph} - I_D - I_{sh} \tag{2.1}$$

Where:

- I_{ph} = photocurrent (proportional to irradiance)
- I_D = diode current
- I_{sh} = shunt leakage current

The diode current is governed by the Shockley diode equation:

$$I_D = I_0 \left(e^{\frac{V+I R_s}{n V_t}} - 1 \right) \tag{2.2}$$

Where:

- I_0 = diode saturation current

- n = diode ideality factor
- $V_t = kT/q$ = thermal voltage
- V = output voltage of PV cell
- I = output current of PV cell
- R_s = series resistance

The shunt current is:

$$I_{sh} = \frac{V + IR_s}{R_{sh}} \quad (2.3)$$

Where:

- R_{sh} = shunt resistance

Thus, the full PV model becomes:

$$I = I_{ph} - I_0 \left(e^{\frac{V+IR_s}{nV_t}} - 1 \right) - \frac{V + IR_s}{R_{sh}} \quad (2.4)$$

This equation describes the I–V curve and forms the basis for MPPT operation.

2.2.2 Photocurrent dependence on irradiation

$$I_{ph} = \left[\frac{G}{1000} \right] (I_{sc,ref} + \alpha(T - 25)) \quad (2.5)$$

Where:

- G = irradiance (W/m^2)
- $I_{sc,ref}$ = reference short-circuit current
- α = temperature coefficient of current
- T = PV cell temperature ($^{\circ}\text{C}$)

2.2.3 PV array power characteristics

The PV Power–Voltage (P–V) curve has a single MPP at:

$$\frac{dP}{dV} = 0 \quad (2.6)$$

Due to changing irradiance and temperature, MPP shifts continuously and requires tracking through MPPT algorithms.

2.2.4 Series and parallel combination

If a single module has:

- Voltage = V_m
- Current = I_m

Then for an array, **Series connection:**

$$V_{array} = N_s \cdot V_m \quad (2.7)$$

Parallel connection:

$$I_{array} = N_p \cdot I_m \quad (2.8)$$

Where N_s and N_p are the number of modules in series and parallel, respectively.

2.3 DC-DC BOOST CONVERTER MODELLING

The PV system uses a DC-DC boost converter to raise the low PV output voltage to the necessary DC-link voltage level for inverter operation. It ensures effective power transfer and steady system operation by serving as an interface between the PV array and the DC-link. Circuit diagram for a DC-to-DC boost converter shown in Fig. 2.3. To extract the maximum amount of solar power possible under various climatic conditions, the boost converter also features MPPT control.

The boost converter's primary purposes are:

- Increasing the voltage of the PV array to the necessary DC-link voltage
- Connecting the PV system to the MPPT controller

An inductor (L), power switch (MOSFET/IGBT), diode, output capacitor (C), and DC-link/load connection make up the majority of the boost converter architecture.

During the switching phase, the inductor stores energy and facilitates voltage boosting. While the diode creates a channel for energy transmission from the inductor to the output while the switch is in the OFF position, the power semiconductor switch controls converter function via controlled switching action.

For seamless system operation, the output capacitor lowers output voltage ripple and keeps the DC-link voltage steady. The DC-link and inverter receive the increased DC output voltage for further power conversion and load delivery. Effective voltage boosting, dependable power transmission, and steady performance of the PV-BESS integrated system under various operating circumstances is made possible by the coordinated functioning of these components.

The DC-DC boost converter's voltage conversion ratio illustrates the connection between the converter's input and output voltages. It assesses the converter's capacity to increase voltage under various duty cycle circumstances. The output voltage may be raised above the input PV voltage by adjusting the switching device's duty cycle. Maintaining the necessary DC-link voltage for steady inverter operation is largely dependent on the voltage conversion ratio. The efficiency of the converter and the overall performance of the system are enhanced by properly designed conversion ratios. The relationship between the DC-DC boost converter's input and output voltages is shown in the equation below. It shows that changing the converter duty cycle may raise the output voltage.

$$V_o = \frac{V_{in}}{1 - D} \quad (2.9)$$

where:

- D = duty cycle (0–1)
- V_o = output voltage of the boost converter
- V_{in} = input voltage from the PV array

The MPPT algorithm adjusts D to operate PV at maximum power.

The inductance value needed to operate the boost converter is determined using the formula below. Smooth current flow and steady converter performance with lower ripple content are guaranteed by appropriate inductance choices.

$$L = \frac{V_{in} (V_{out} - V_{in})}{f_{sw} * V_{out} * \Delta I_L} \quad (2.10)$$

where:

- L = inductance of the boost converter
- ΔI_L = inductor current ripple
- f_{sw} = switching frequency

The necessary inductance value for sustaining Continuous Conduction Mode (CCM) operation and minimizing current ripple in the boost converter is found using this formula.

The boost converter's output capacitance is determined using the following formula. During converter operation, choosing the right capacitance helps to reduce voltage ripple and maintain a steady output voltage.

$$C = \frac{I_{out} (V_{out} - V_{in})}{f_{sw} * V_{out} * \Delta V_{out}} \quad (2.11)$$

where:

- C = capacitance of the boost converter
- ΔV_{out} = output voltage ripple
- ΔI_{out} = output current of the converter

The DC-DC boost converter design used in the proposed system is provided in **Appendix 2**. It includes the converter configuration and parameter calculation.

The necessary capacitor value for lowering output voltage ripple and preserving a steady DC-link voltage in the boost converter is found using this formula. Fig. 2.3 shows the circuit diagram of the DC-DC boost converter used in the proposed PV system. The converter boosts the low PV output voltage to the required DC-link voltage level for stable system operation.

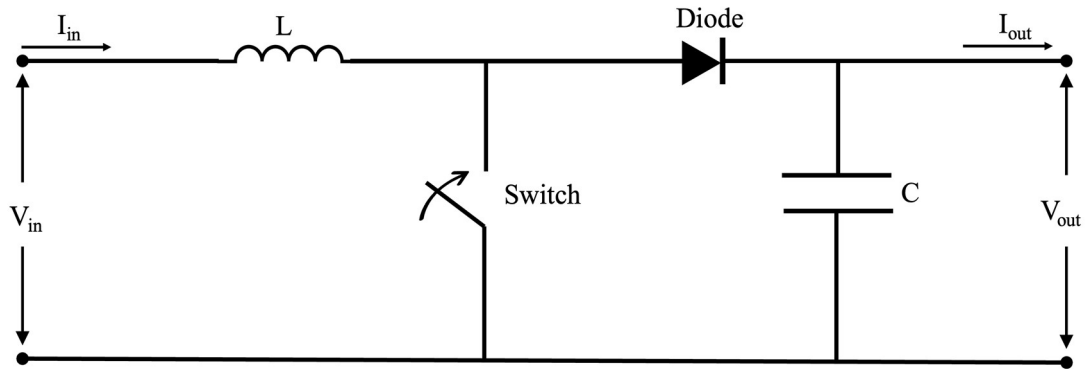


Fig. 2.3 Circuit diagram for a DC-to-DC boost converter

2.4 BATTERY ENERGY STORAGE SYSTEM (BESS) MODELLING

In order to provide steady and uninterrupted power delivery under fluctuating solar generation and load situations, the BESS is a crucial part of the grid-connected PV system. A lithium-ion battery is taken into consideration in this work because of its high energy density, extended cycle life, low maintenance needs, and excellent charging–discharging efficiency. When there is high irradiance, the BESS saves extra energy produced by the PV system. When there is low PV generation or an increase in load demand, the stored energy is released. This promotes stable functioning of the entire PV–BESS integrated system and increases system dependability and power quality.

State of Charge (SOC), battery voltage characteristics, and efficiency parameters are used to analyze the battery system performance. These models facilitate efficient battery energy management and aid in comprehending battery behavior during charging and discharging activities.

2.4.1 State of charge (SOC) model

The battery's usable energy stored as a proportion of its rated capacity is represented by the State of Charge (SOC). It is a key measure for keeping monitoring on battery performance and upholding safe operating boundaries. The battery's SOC is computed as follows:

$$SOC(t) = SOC(0) - \frac{1}{C_{rated}} \int i_{bat}(t) dt \quad (2.12)$$

where:

- C_{rated} = rated battery capacity (Ah)

- $i_{bat}(t)$ = battery current
- $SOC(t)$ = State of charge at time t
- $SOC(0)$ = Initial state of charge

While a positive **battery** current indicates discharging operation, which results in a fall in SOC, a negative battery current shows charging operation, which causes an increase in SOC.

2.4.2 Battery Voltage Model

The battery voltage characteristics are represented using a nonlinear mathematical model given by:

$$V_{bat} = E_0 - Ri_{bat} - K \ln(Q - q(t)) \quad (2.13)$$

where:

- E_0 = open-circuit voltage
- R = internal resistance
- $q(t)$ = extracted charge from the battery
- Q = battery capacity
- i_{bat} = battery current
- V_{bat} = battery terminal voltage

2.4.3 Battery efficiency

The efficiency of energy transfer and storage during charging and discharging procedures is represented by battery efficiency. The charging and discharging efficiencies are expressed as:

$$\eta_c = \frac{\text{Energy stored}}{\text{Energy supplied}} \quad (2.14)$$

$$\eta_d = \frac{\text{Energy delivered}}{\text{Energy extracted}} \quad (2.15)$$

Round-trip efficiency:

$$\eta = \eta_c * \eta_d \quad (2.16)$$

Lithium-ion batteries are ideal for storage systems that rely on RES since they typically offer excellent round-trip efficiency in the region of 92–96%.

2.5 BIDIRECTIONAL DC–DC CONVERTER MODELLING

The bidirectional DC–DC converter is used to interface the BESS with the DC-link of the grid-connected PV system. During charging and discharging processes, it permits regulated power flow between the battery and the DC-link. Depending on the needs of the system and the state of the power balance, the converter runs in two distinct modes.

2.5.1 Buck mode (Charging mode):

When in buck mode, the converter uses the extra power at the DC-link to charge the battery by acting as a step-down converter. Power is transferred from the DC-link to the battery storage system in this mode. The battery charging voltage is controlled by adjusting the duty cycle of the converter switch.

The battery charging voltage is given by:

$$V_{bat} = D * V_{dc} \quad (2.17)$$

Charging current is expressed as:

$$i_{bat} = \frac{V_{dc} - V_{out}}{R} \quad (2.18)$$

Where:

- V_{bat} = battery voltage
- V_{DC} = DC-link voltage
- R = circuit resistance

2.5.2 Boost mode (Discharging mode)

In boost mode, when PV generation is low or load demand is high, the converter functions as a step-up converter to transfer stored battery energy to the DC-link. In order

to sustain steady system operation and continuous power delivery, electricity is transferred from the battery to the DC-link in this mode.

When discharging, the DC-link voltage is determined by:

$$V_{dc} = \frac{V_{bat}}{1 - D} \quad (2.19)$$

The battery discharging current is expressed as:

$$i_{bat} = \frac{V_{bat} - (1 - D)V_{dc}}{R} \quad (2.20)$$

2.6 VOLTAGE SOURCE INVERTER (VSI) MODELLING

A crucial component of the grid-connected PV-BESS is the VSI, which converts DC power at the DC-link into synchronized three-phase AC power that supplies the load and interfaces with the utility grid. For steady and dependable power transfer, the inverter makes sure that the PV-BESS system and the grid are properly synchronized in terms of voltage, frequency, and phase angle. The VSI carries out some crucial control tasks in addition to DC-AC conversion to enhance system performance and power quality. The inverter minimizes harmonic distortion in the output current, maintains the correct power factor, and controls active and reactive power flow in accordance with load and grid requirements. To achieve stable inverter operation and efficient grid integration, advanced control techniques like Phase-Locked Loop (PLL) synchronization, dq-axis current regulation, and pulse width modulation (PWM) are frequently employed. As a result, the VSI is essential for preserving system stability, enhancing power quality, and guaranteeing uninterrupted power delivery to the linked load.

Furthermore, the VSI enables bidirectional power flow between the PV-BESS system and the utility grid, enabling efficient utilization of available energy under a variety of operating conditions. Through stable inverter operation and suitable grid synchronization, the VSI ensures a reliable and continuous power supply to the related

load while supporting overall system stability and energy management. Additionally, by responding dynamically to sudden changes in demand and fluctuations in PV production, the inverter keeps the system's power flow balanced. Furthermore, the VSI improves the overall operating flexibility of the PV–BESS integrated system and makes it easier to employ renewable energy resources, as shown in **Fig. 2.4**. Six power semiconductor switches stacked in a three-phase bridge arrangement make up the Voltage Source Inverter (VSI). The DC-link voltage is converted into a three-phase AC output voltage by these switches, which are typically implemented using IGBTs or MOSFETs and run in complementary pairs. The controller board generates Pulse Width Modulation (PWM) gate pulses that regulate the inverter's switching action. The VSI controls the output voltage, current, active power, and reactive power delivered to the AC load and utility grid by managing the inverter switches' duty cycle and switching sequence. Stable inverter operation, less harmonic distortion, and synchronized power transmission with the grid are other benefits of proper switching management.

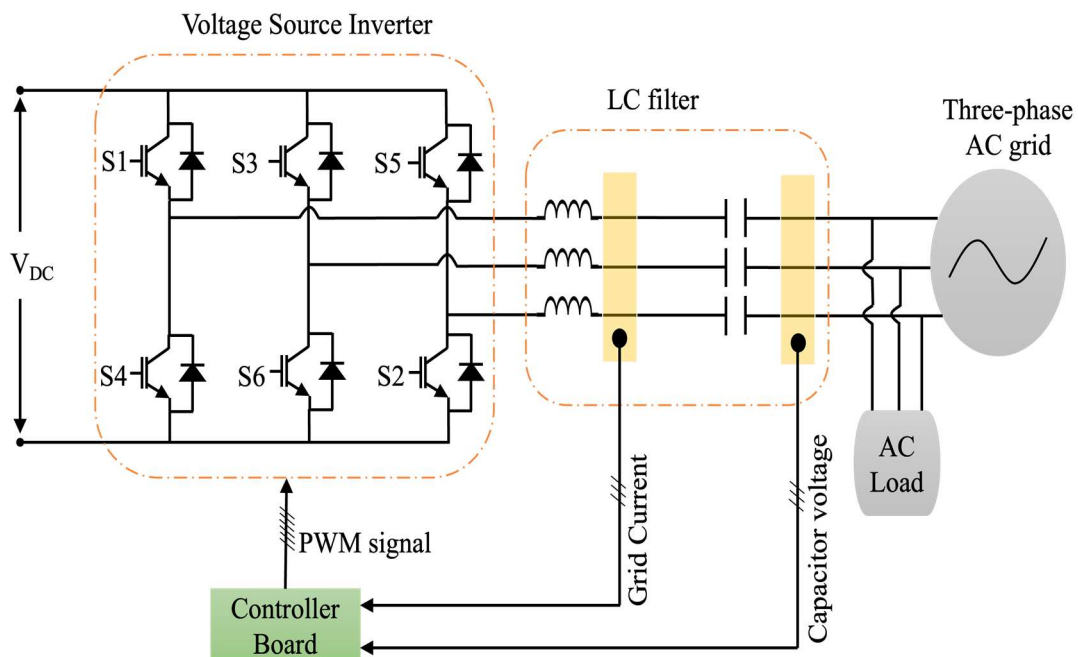


Fig. 2.4 Grid-connected VSI

2.6.1 Clarke transformation

Three-phase variables in the ABC reference frame are transformed into a two-axis stationary orthogonal reference frame using the Clarke (α - β) transformation. Since the

sum of **the** three-phase quantities in a balanced three-phase system is zero, the system can be represented by just two independent components. While maintaining the fundamental electrical properties, this transformation makes mathematical study and management of three-phase systems easier. Three-phase currents (i_a, i_b, i_c) are transformed by the Clarke transformation into stationary-frame components (i_α, i_β), which are simpler to handle in control applications such as vector control systems and inverter management.

The Clarke transformation is expressed as:

$$\begin{bmatrix} i_\alpha \\ i_\beta \end{bmatrix} = \frac{2}{3} \begin{bmatrix} 1 & -\frac{1}{2} & -\frac{1}{2} \\ 0 & \frac{\sqrt{3}}{2} & -\frac{\sqrt{3}}{2} \end{bmatrix} \begin{bmatrix} i_a \\ i_b \\ i_c \end{bmatrix} \quad (2.21)$$

Where:

- i_a, i_b, i_c = Three-phase currents in abc reference frame
- i_α, i_β = Stationary frame current components

2.6.2 Park transformation

The Park Transformation creates a revolving dq reference frame that is in sync with the grid frequency from the stationary α - β frame variables. Under steady-state conditions, this transformation transforms sinusoidal AC data into DC-like quantities, simplifying and improving current, voltage, and power regulation. The d -axis component primarily regulates active power in the dq frame, whereas the q -axis component regulates reactive power. In grid-connected inverter systems, this allows independent and decoupled control of both active and reactive power.

The Park transformation is given by:

$$\begin{bmatrix} i_d \\ i_q \end{bmatrix} = \begin{bmatrix} \cos \theta & \sin \theta \\ -\sin \theta & \cos \theta \end{bmatrix} \begin{bmatrix} i_\alpha \\ i_\beta \end{bmatrix} \quad (2.22)$$

Where:

- i_d = Direct-axis current component

- i_q = Quadrature-axis current component
- θ = Grid or synchronous reference frame angle

In order to increase system stability and dynamic performance, vector control and grid synchronization approaches frequently employ the Park transformation.

CHAPTER 3

CONTROL STRATEGIES

3.1 INTRODUCTION

Control techniques are critical to ensuring that the grid-connected PV- BESS operates consistently, reliably, and efficiently. The output power of the system constantly fluctuates over time because solar PV generation is highly dependent on environmental factors like temperature and solar irradiation. Variations in load demand and grid circumstances further increase the complexity of system functioning. Therefore, to maintain steady power flow, control system voltage, oversee battery operation, and guarantee continuous power delivery to the linked load, an efficient and well-coordinated control framework is needed.

The main control strategies utilized in the suggested PV–BESS integrated system are presented in this chapter, including Grid-Side Inverter Control, DC-Link Voltage Control, Battery Charge–Discharge Control, and MPPT. Together, these control techniques enable optimal solar power extraction, effective battery energy management,

reliable DC-link operation, appropriate grid synchronization, and enhanced power quality. Under various load and climatic situations, the coordinated application of these control techniques improves overall system stability, dependability, and compliance with grid operating criteria.

3.2 MAXIMUM POWER POINT TRACKING (MPPT) CONTROL

A PV array's output characteristics are nonlinear and constantly fluctuate in response to variations in temperature and solar light. Because of this, the PV system operating point also varies constantly, necessitating the use of an efficient MPPT method to guarantee maximum power extraction in all environmental circumstances. Because MPPT increases energy harvesting efficiency and boosts overall system performance, it is a crucial control approach for PV systems.

Due to its high tracking accuracy, quick dynamic reaction, and less steady-state oscillations than traditional Perturb and Observe (P&O) techniques, the Incremental Conductance (INC) algorithm is chosen for MPPT control in this work. By calculating the slope of the power-voltage (P-V) curve, the INC method establishes the operating point's location in relation to the MPP. Appendix 1 contains the MATLAB/Simulink code used to develop the MPPT control method. The designed control algorithm for maximizing solar power extraction under various environmental situations is included in the appendix. The rate at which power changes in relation to voltage reaches zero at the maximum power point. In order to maintain operating at the MPP and optimize solar power extraction, the controller continuously modifies the DC–DC boost converter's duty cycle. The operating conditions of the INC algorithm are given by:

$$\frac{dP}{dV} = 0 \text{ for } V = V_{mpp} \quad (3.1)$$

$$\frac{dP}{dV} > 0 \text{ for } V < V_{mpp} \quad (3.2)$$

$$\frac{dP}{dV} < 0 \text{ for } V > V_{mpp} \quad (3.3)$$

The MPPT control system's block design is displayed in Fig. 3.1. The INC algorithm continually measures and processes the PV voltage (V_{PV}) and PV current (I_{PV}). The controller creates the proper gate pulses for the PWM generator to regulate the boost converter's switching activity based on these readings. The MPPT controller maintains the PV array's MPP under fluctuating solar irradiation and temperature conditions by continually modifying the converter duty cycle. According to the duty cycle supplied by the INC algorithm, the PWM generator generates switching pulses for the boost converter switch. This switching procedure enables maximum solar power extraction and also regulates the boost converter's output voltage. Thus, inside the PV–BESS integrated system, the MPPT control system enhances overall energy conversion efficiency, sustains steady converter performance, and facilitates dependable power transmission.

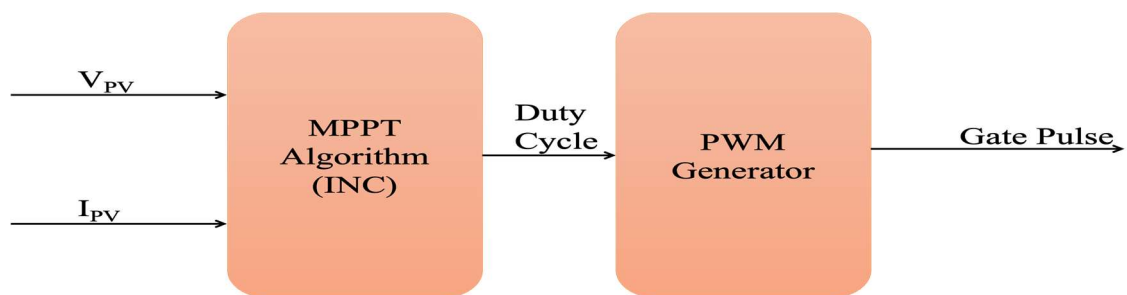


Fig. 3.1 Block diagram for MPPT control

The duty-cycle-based Incremental Conductance MPPT algorithm flowchart is shown in Fig. 3.2. In order to ensure operation at the MPP under changing environmental conditions, the controller continuously analyzes the current and past values of PV voltage and current, compares the operating conditions, and modifies the converter duty cycle as necessary.

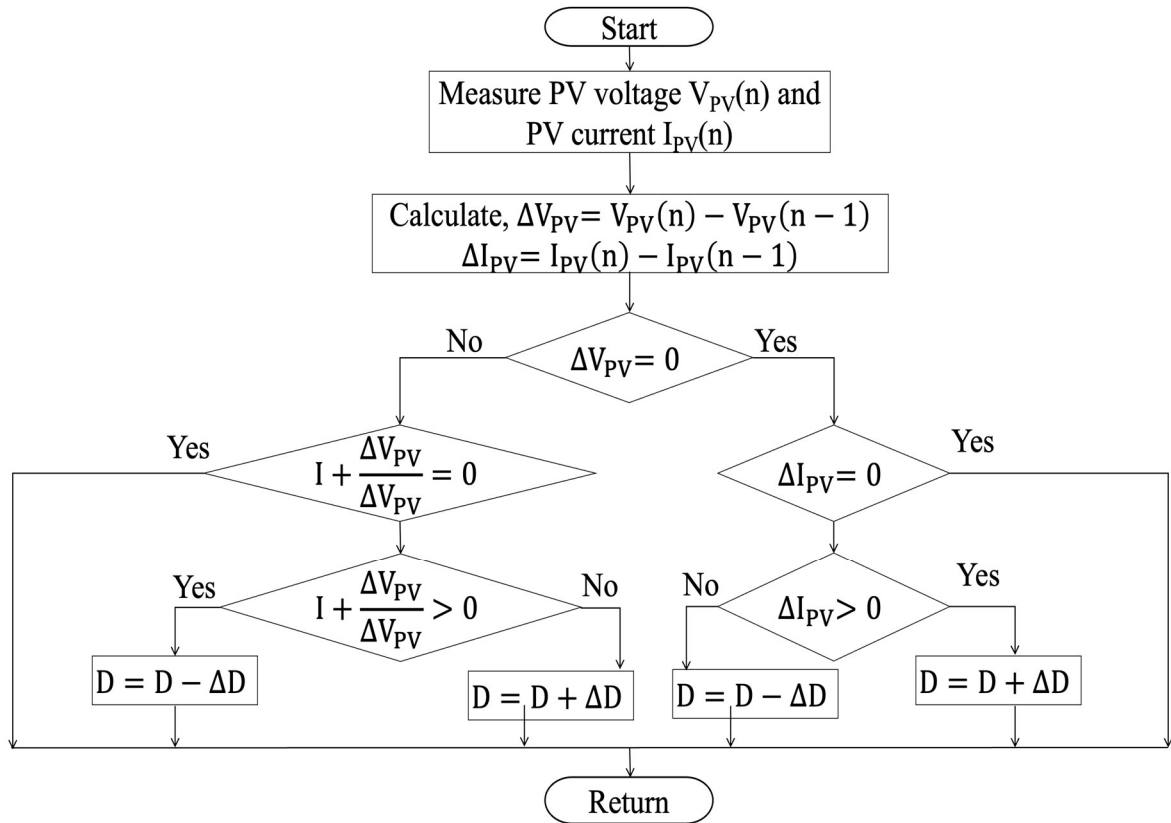


Fig. 3.2 Duty cycle control algorithm of IC for MPPT

3.3 BATTERY CHARGE–DISCHARGE CONTROL

The BESS plays a crucial role in compensating for PV intermittency and ensuring continuous power delivery. Its operation requires an intelligent control strategy that manages charging and discharging based on the State of Charge (SOC), power balance, and system constraints. When PV generation exceeds load demand, the surplus power charges the battery, provided the SOC is below its predefined upper limit. Conversely, when PV power is insufficient, the battery discharges to support the DC-link voltage and maintain power flow to the grid or load.

The bidirectional DC–DC converter regulates battery current in both charging (buck mode) and discharging (boost mode) operations. SOC-based protection mechanisms prevent battery overcharging and deep discharge, enhancing battery lifespan and system reliability. The coordinated control of PV and BESS ensures smooth energy transitions,

reduces stress on the power electronics, and maintains overall system stability during varying operating conditions.

TABLE 3.1. The battery parameters

Parameters	Value
Nominal Voltage	400 V
Rated Capacity	48 Ah
State of Charge (SOC)	80 %

3.4 DC-LINK VOLTAGE REGULATION

A stable DC-link voltage is essential for reliable inverter operation and high-quality AC waveform generation. Variations in PV output or battery power can destabilize the DC bus; therefore, a closed-loop control scheme is employed to regulate the DC-link voltage at a constant reference value. A Proportional–Integral (PI) controller is used to adjust the duty cycle of the boost converter or battery converter depending on system dynamics. When the DC-link voltage drops due to sudden load variations or reduced PV generation, the controller increases power input from the battery or adjusts the PV boost converter. If the voltage rises, the controller reduces power extraction or directs more power into the battery. This control ensures that the inverter receives a stable DC supply, preventing overvoltage, undervoltage, and potential system shutdowns. Maintaining a regulated DC-link is also essential for ensuring low total harmonic distortion (THD) on the AC side.

3.5 GRID-SIDE INVERTER AND SYNCHRONIZATION CONTROL

The grid-side inverter is responsible for injecting high-quality AC power into the utility grid while maintaining grid code compliance. Using dq-axis current control, the inverter independently regulates active and reactive power. By aligning the d-axis with the grid voltage vector, active power is controlled through the d-axis current component, whereas reactive power is controlled by the q-axis component. This ensures precise control of power flow while minimizing harmonics and maintaining power factor requirements.

Synchronization with the grid is achieved using a Phase-Locked Loop (PLL), which extracts the instantaneous phase angle and frequency of the grid voltage. The

synchronous reference frame PLL (SRF-PLL) is applied due to its robustness and fast dynamic response. Accurate synchronization ensures smooth power injection, prevents circulating currents, and enables seamless operation during grid disturbances. The integrated control structure of the inverter, dq current control, and PLL ensures that the PV–BESS system operates reliably under normal and fluctuating grid conditions.

In this type of control, signal references are computed based on the power requirement. m_d and m_q refer to the predicted voltages stated in the equations.

$$\mathbf{m}_d = U_d - \omega L i_q + v_d \quad (3.4)$$

$$\mathbf{m}_q = U_d - \omega L i_d \quad (3.5)$$

Where, U_d and U_q are given as

$$U_d = (K_{p1} + \frac{K_{i1}}{s})e_d \quad (3.6)$$

$$U_q = (K_{p2} + \frac{K_{i2}}{s})e_q \quad (3.7)$$

where, e_d and e_q are defined as

$$e_d = i_{d_ref} - i_d \quad (3.8)$$

$$e_q = i_{q_ref} - i_q \quad (3.9)$$

The dq-axis current control arrangement for the grid-connected VSI is shown in Fig. 3.3. The PWM generator generates switching pulses for grid synchronization and steady inverter operation, while the controller employs PI regulators in the dq reference frame to individually regulate active and reactive current components.

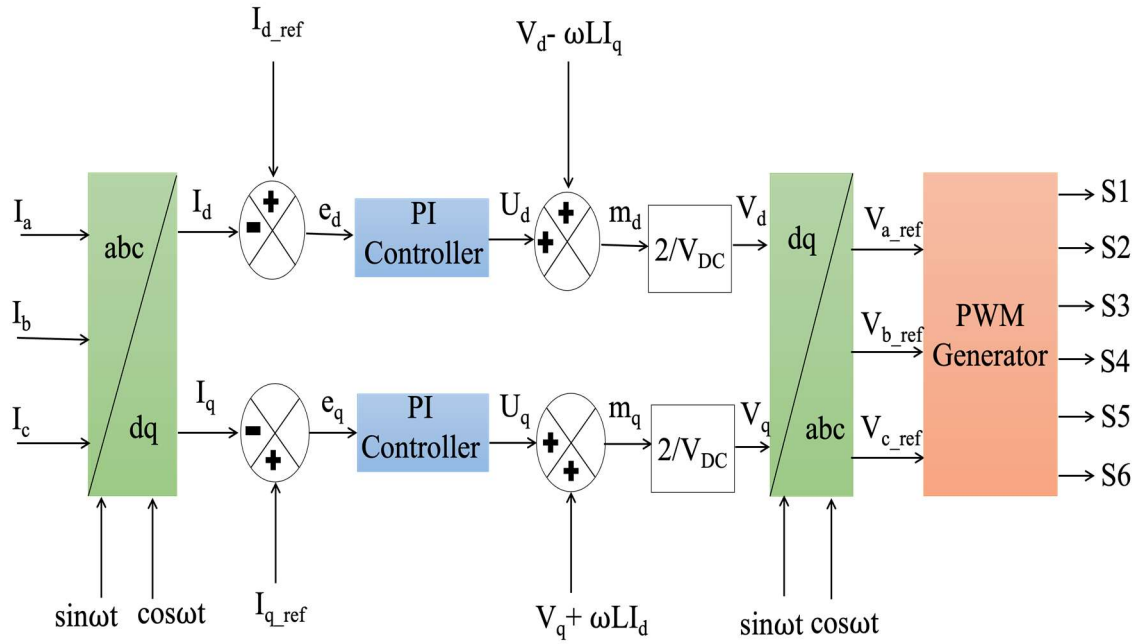


Fig. 3.3 Block diagram for inverter control

CHAPTER 4

SIMULATION RESULTS AND DISCUSSION

4.1 INTRODUCTION

The simulation results and performance analysis of the suggested three-phase grid-connected PV system supported by the BESS and created in the MATLAB/Simulink environment are presented in this chapter. A PV array, DC-DC boost converter with

MPPT, BESS with bidirectional converter, DC-link capacitor, three-phase VSI, dq-axis control system, Phase-Locked Loop (PLL) synchronization, and grid interface via an LC filter make up the entire system. Effective energy conversion and reliable system performance under various circumstances are ensured by the coordinated action of these components.

The main goal of the suggested PV-BESS integrated system is to meet fluctuating power demand requirements while supplying a steady and continuous power supply to the associated load. As a result, the system's performance is assessed under various operating scenarios, including variations in solar irradiation, abrupt load fluctuations, battery charging and discharging transitions, and grid synchronization settings. Voltage stability, DC-link regulation, inverter response, power flow management, battery performance, and overall system dependability are all examined in relation to the simulation results. The collected findings show how well the suggested control strategies work to maintain steady power delivery and guarantee dependable PV-BESS integrated system functioning.

4.2 RESULTS

Fig. 4.1 shows the irradiation provided to the PV. This curve has a variety of irradiation values up to 1000 W/m². Furthermore, Fig. 4.2 shows the PV voltage and the PV current as 460.5 V and 16.3 A, respectively. Finally, Fig. 4.3 displays the boost converter voltage and the boost converter current output results, respectively. It is due to the MPPT method's nature in PV that it provides information about the control behavior.

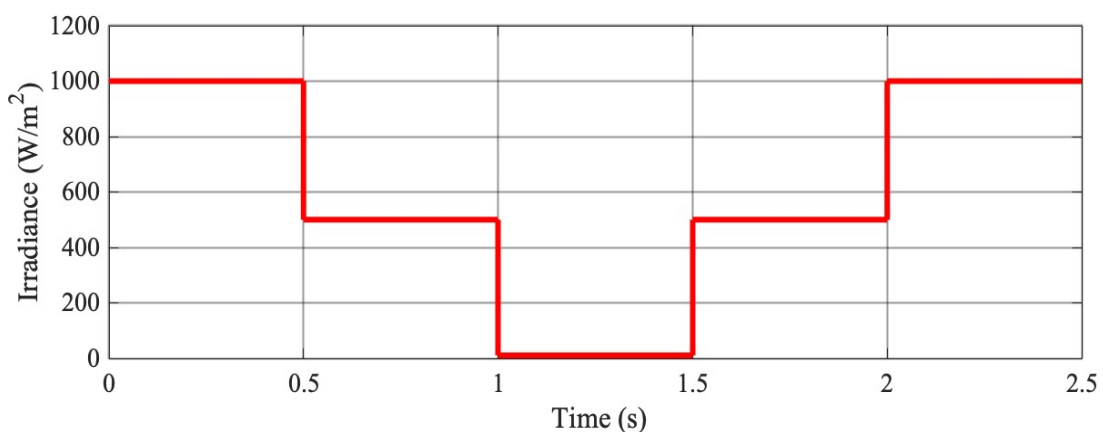


Fig. 4.1 Variable Solar Irradiance Profile

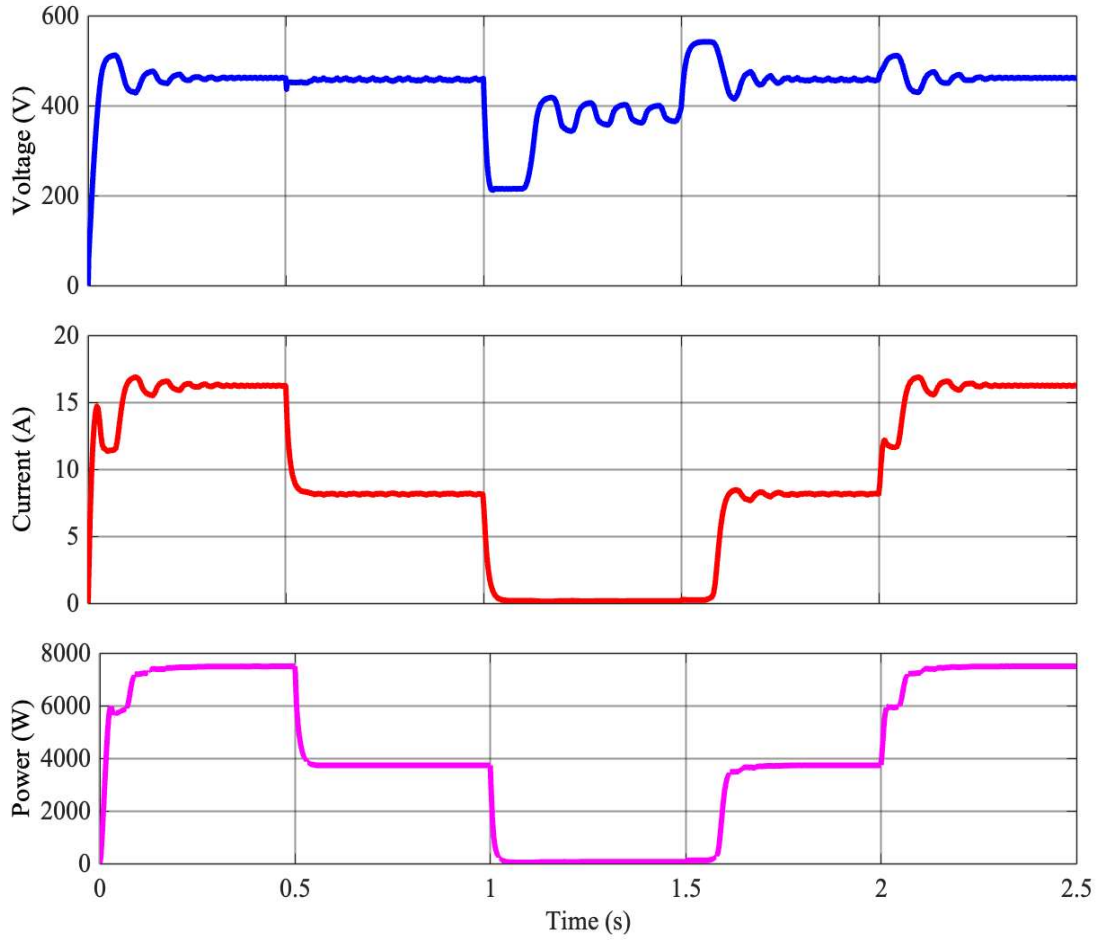


Fig. 4.2 Voltage, current and power of PV

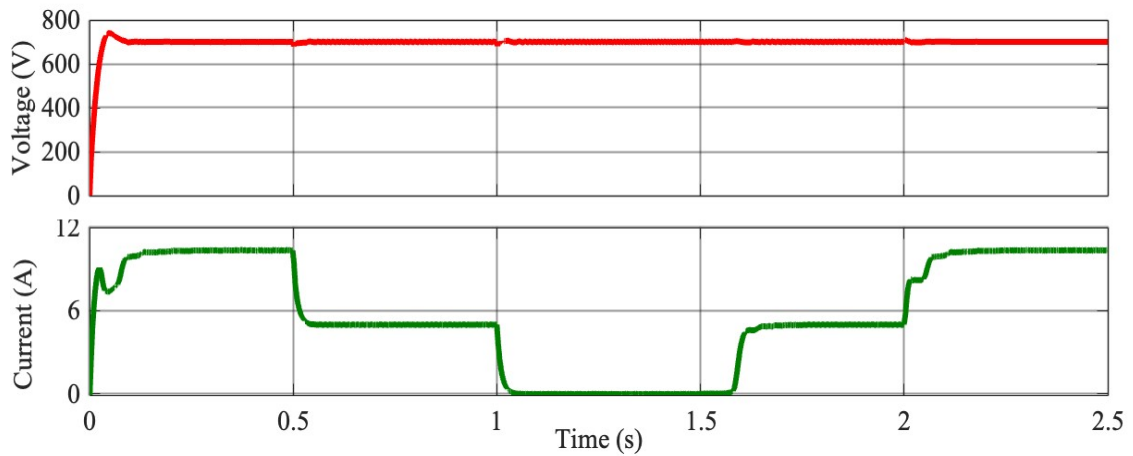


Fig. 4.3 Boost converter voltage and current.

The BESS’s bidirectional operation is crucial in controlling power flow for varying solar irradiance. An examination of Table 3.1 indicates that the nominal battery voltage is 400 V. The major modes of the system are either charging or discharging.

Charging Mode: The system is charging when solar irradiance is high at 1000 W/m²; this is to store excess energy. From Fig. 4.4, the battery also charges similarly with terminal voltage and current at 436 V and -7.4 A, respectively; the negative sign indicates charging and battery SOC% increase at this point.

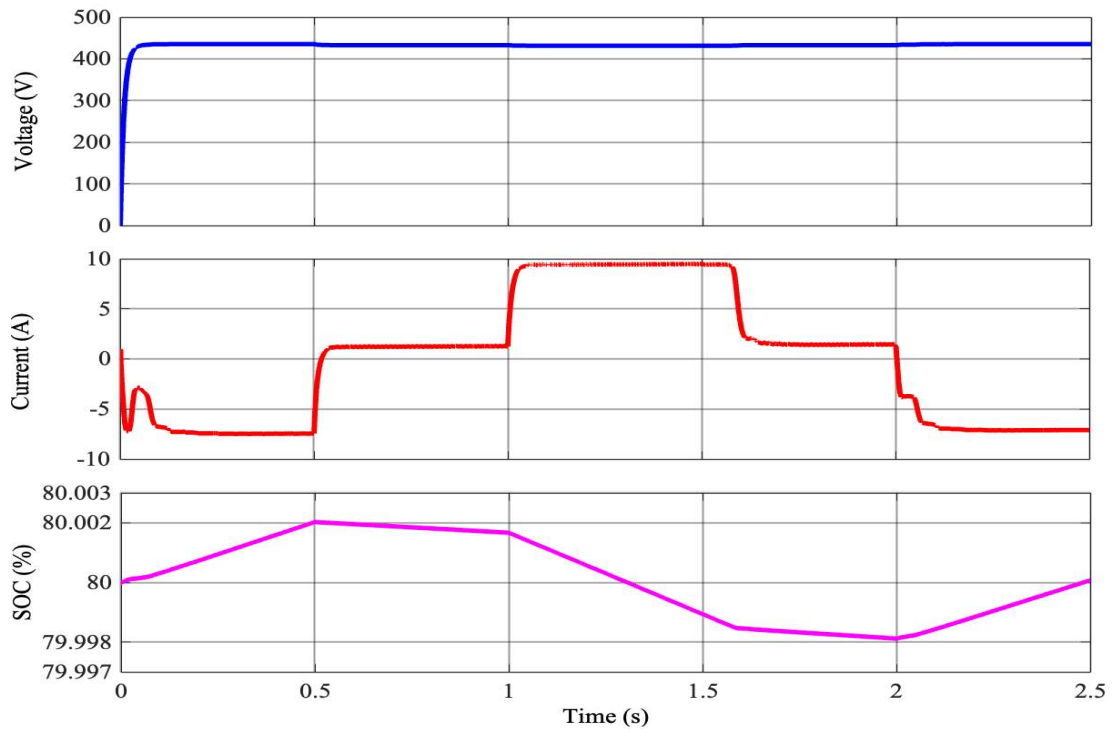


Fig. 4.4. Battery Voltage, Battery Current and SOC %

The performance study of the suggested PV–BESS integrated system under various solar irradiance circumstances is shown in Table 4.1. The findings demonstrate that although the DC-link voltage stays constant at the intended level, the PV voltage, current, and produced power fluctuate in response to variations in sun irradiation. Additionally, it is noted that the BESS maintains a constant power supply to the load by operating in charging mode during high irradiance situations and switching to discharging mode during low irradiance conditions. The outcomes shown in Table 4.1 attest to the efficiency of the control mechanisms put in place in preserving steady and dependable system performance in the face of changing external circumstances.

TABLE 4.1 System Response Under Different Solar Irradiance Levels

Solar Irradiance (W/m ²)	PV Voltage (V)	PV Current (A)	PV Power (W)	DC-Link Voltage (V)	DC-Link Current (A)	Battery Mode
1000	460.5	16.3	7500	700	10.38	Charging
500	390–400	8–8.5	3200–3500	700	4.5–5	Mild Charging
10	220–230	0.2–0.5	40–100	700	1.2	Discharging
500	390–400	8–8.5	3200–3500	700	4.5–5	Reduced Discharging
1000	460.5	16.3	7500	700	10.38	Charging

Discharging Mode: At the same time, with an extremely low level of solar irradiance discharge, let us say 10 W/m², the battery discharges to level the system. As illustrated in Fig. 4.4, the battery outputs 9 A to the DC link at a terminal voltage of 436 V. This procedure is crucial for the DC link’s synchronization. To achieve this, the battery controller employs a 700 V V_{Ref} and a 700 V fixed DC link voltage. This discharge reacts to the decrease of the PV current I_{PV} accelerated by the low irradiance, which implies that since PV out is low, little current is available for the inverter’s needs to lower to maintain a stable current supplied to the inverter and then to the grid. The battery SOC (%) deteriorates during this stage. This is followed by PLL, which estimates the phase and frequency of the input voltage. The PLL in this system is used to calculate the V_d component for an input RMS voltage of 400 V, and the V_q component is assumed to be zero hence, the angular frequency ω , which is then determined by the grid frequency f . The grid frequency used for the standard is 50 Hz, and the angular frequency is given by $\omega = 2\pi \cdot f = 314$ rad/s. Furthermore, the unit vectors for the phase values are estimated using a harmonic oscillator, as illustrated in Fig. 4.5. These are necessary for calculating the sinusoidal signals that are to be generated at the right phase for synchronization and other usage in the grid.

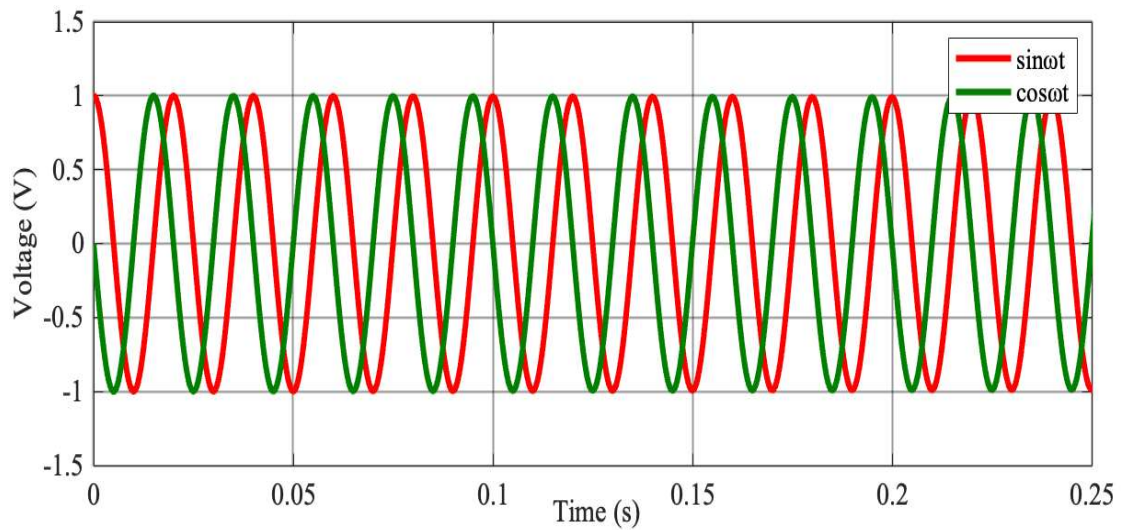


Fig. 4.5 Unit Vector.

Fig. 4.6 shows DC bus current measurements at a high irradiance (1000 W/m^2) instant point DC bus establishes the efficient power flow and distribution. The boost converter reduces the 15 A current from the PV array to 10.38 A. It then accurately distributes the current among the elements of the system. The DC load takes 3.5 A, and the battery charges take the remaining 4.38 A. The inverter is fed by 2.43 A. The total of these currents is perfectly equal to the 10.38 A that flows and proves an efficient power balance and effective current management system. Stable power flow under changing irradiance circumstances is ensured by the utility grid, PV system, and BESS operating in unison. In addition to supporting continuous power supply to the linked load, this power-sharing technique increases system dependability.

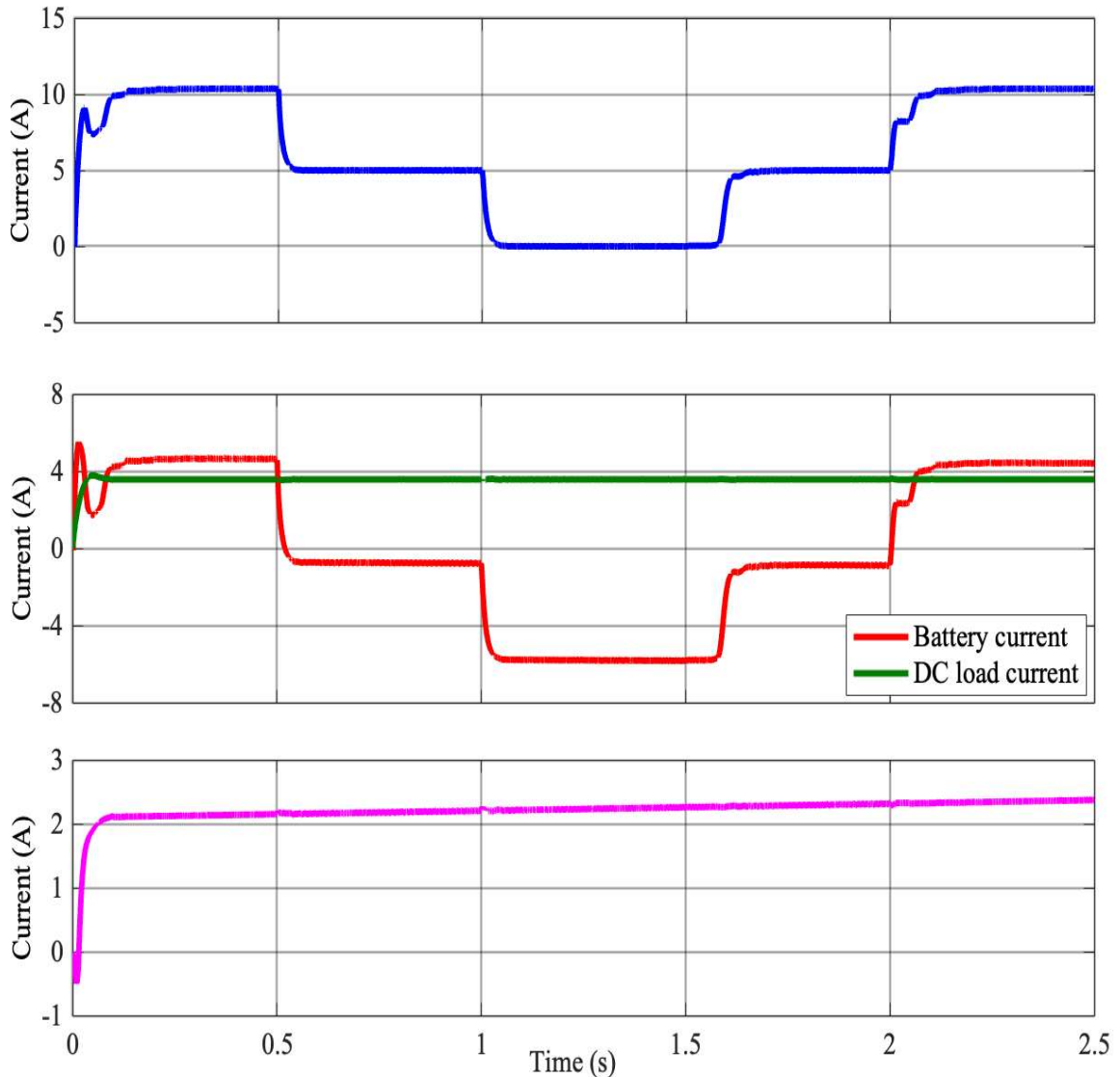


Fig. 4.6 The DC bus current measurements: Boost converter current, Current drawn by battery and DC load, and Inverter current

DC Load: Another power configuration connected to a 196ohm resistive load supplied by the DC link and powered by a high voltage boost converter is shown in Fig.4.7. When the DC Link maintains the constant voltage of 700 V, the power source remains stable, and the load draws a current of 3.5 A, making the power approximately 2500 W. The figure above illustrates the DC load, indicating the power delivered from the Boost converter to the DC load. The setup is common in various industrial applications where the DC voltage cannot be reduced and supports the resistive load at higher steady states. The figure further illustrates the converter’s potential to step up the voltage; hence, the system’s performance is defined by its high-power transfer efficiency.

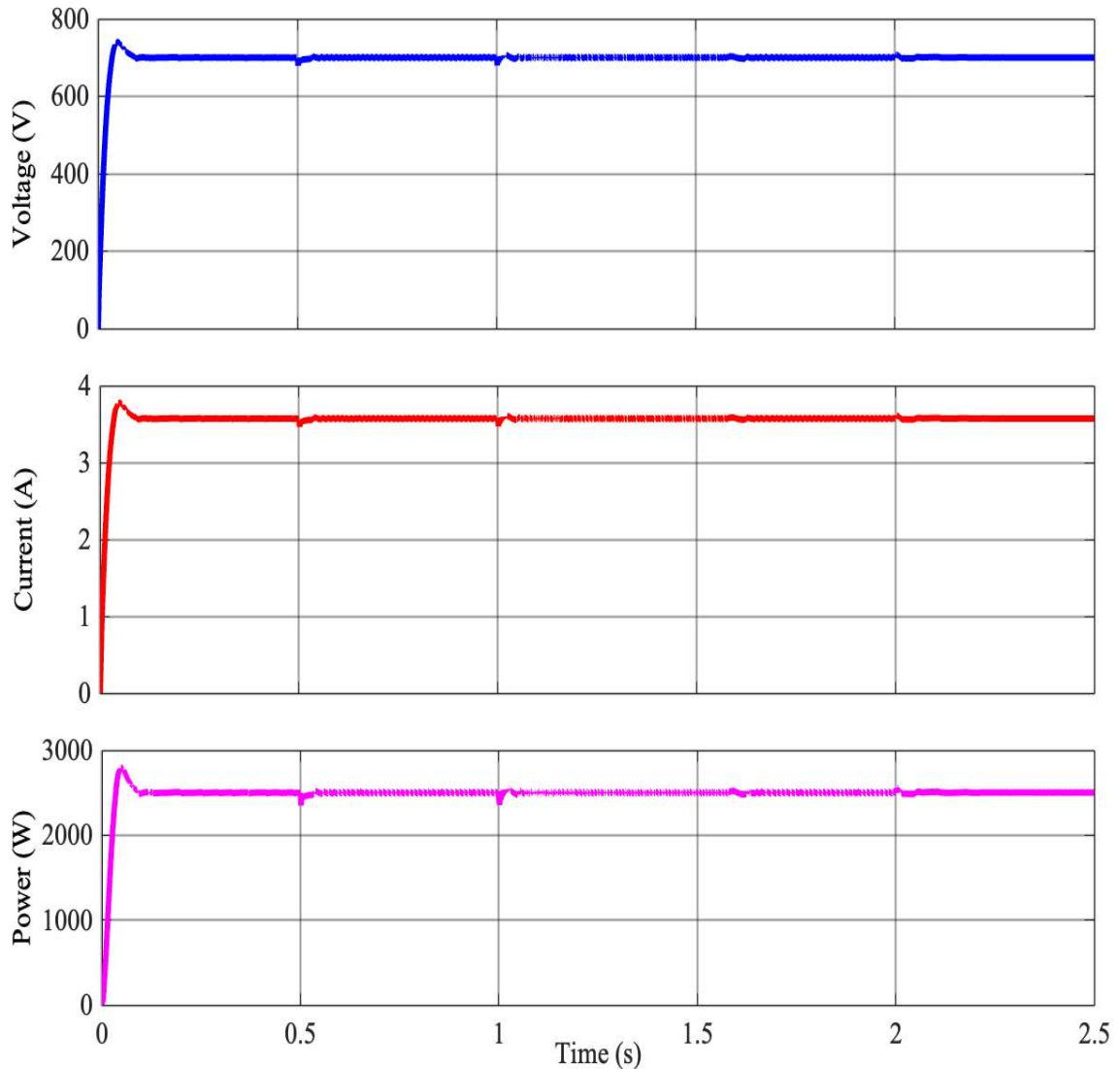


Fig. 4.7 DC load voltage, current, and power

AC Load: An AC Load that draws 2000 W of power is linked between the inverter and power grid. The AC voltage and current waveforms measurements of the load are shown in Fig. 4.8. The peak line value of voltage and current taken was 567 V and 4.1 A, respectively. The measurement ensured that the power is being consumed by the AC load in the Inverter-Grid-PV system. The performance of the load is extremely essential in finding the total efficiency and power flow. The measured data give the specific electrical aspects of the load.

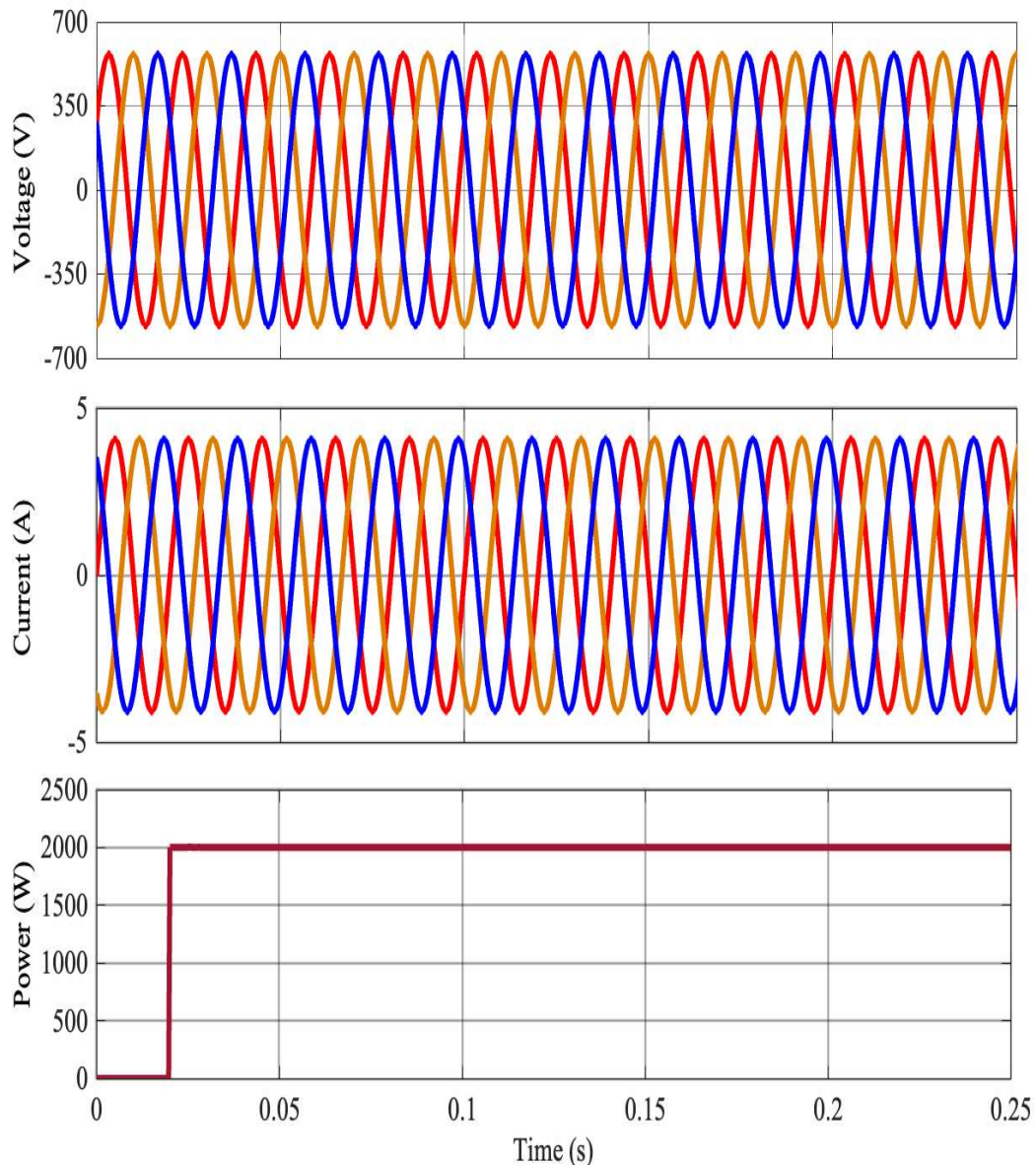


Fig. 4.8 AC load voltage, current, and power

The system operation commences with a PV array that feeds in 7,500 W of power, which is then put through a boost converter and converted the power into a regulated output of 7,000 W. After the power conversion, the output power is then utilized in a strategic approach as per the various load and storage requirements. In this case, a DC load of 2,500 W is embedded by the power output, while a further 3,000 W is used to charge a battery, thus allows storage of energy and utilization during a period of low solar insolation, and the remaining 1,500 W is linked to an inverter that is connected to the AC load source. By adopting the hybrid power supply arrangement, the AC load is fully backed up at all times. The system operational stability is guaranteed by ensuring the

grid peak voltage is kept at 330 V . In addition, the system dynamic current nature plotted in Fig. 4.9 demonstrates the grid supplying current peaking at 1.2 A and the inverter supplying a peak of 3 A. These metrics demonstrate the system's capability in efficient power flow and voltage stability while maintaining a balance of power flow from the PV source and the grid.

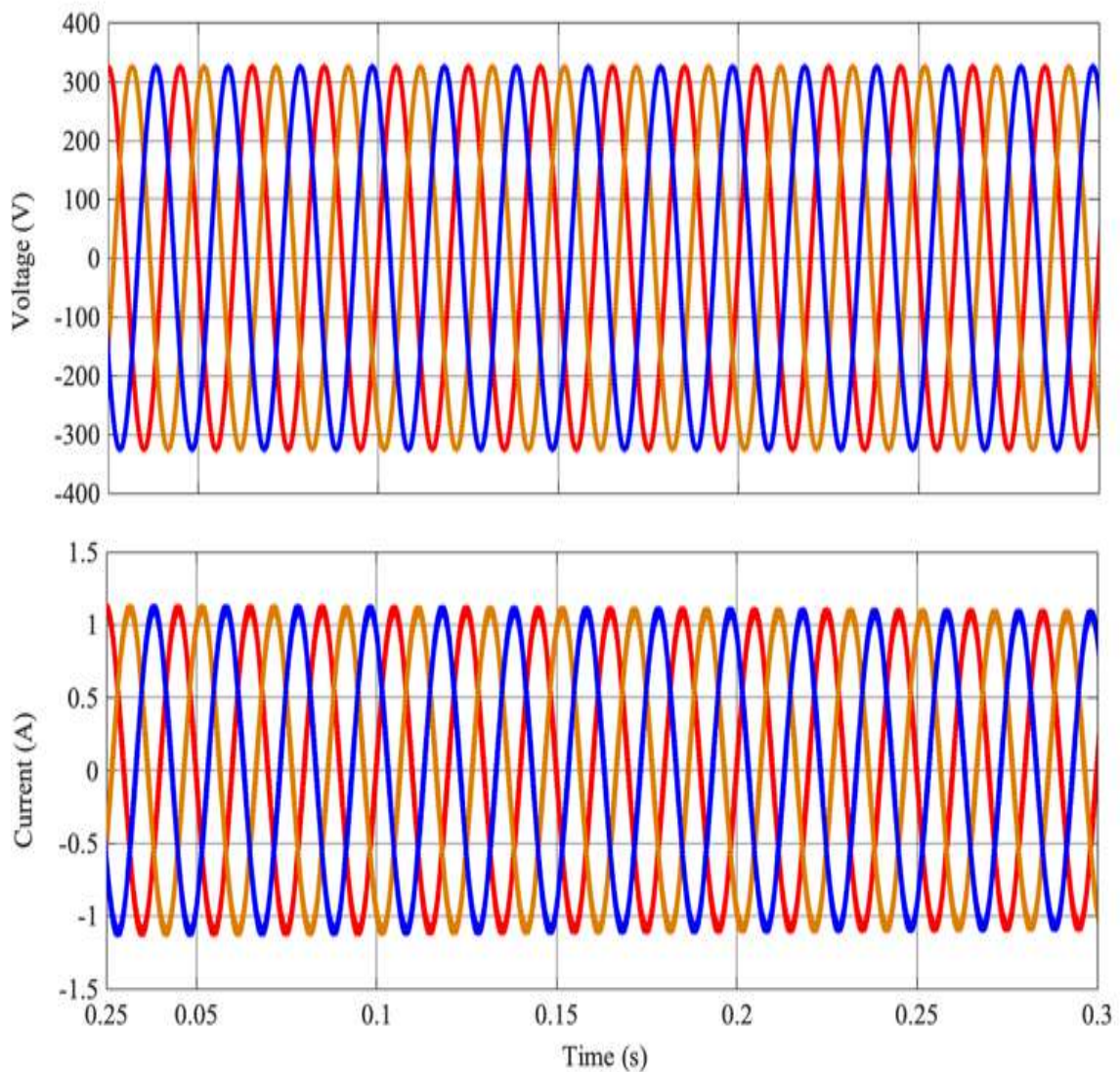


Fig. 4.9 Grid voltage and grid current

The AC load source that has a demand capacity of 2,000 W incorporates an available 1,500 W from the inverter, of the remaining 500 W is sourced from the utility grid. Fig. 4.10 shows the power-sharing performance of the proposed PV-BESS integrated system among the inverter, utility grid, and connected AC load. It can be observed that the inverter power increases gradually to satisfy the load demand, while the grid power

contribution decreases with time. The results demonstrate effective power management and stable coordination between the PV-BESS system and the utility grid for continuous power supply to the load. The power allocation between the inverter, utility grid, and AC load under various solar irradiation scenarios is shown in Table 4.3. The findings show that the PV-BESS system and the utility grid can operate in sync to provide steady power management and continuous load supply.

TABLE 4.2 Power Sharing Under Variable Irradiance

Solar Irradiance (W/m ²)	Inverter Power (W)	Grid Power (W)	AC Load Power (W)	System Observation
1000	1500	500	2000	High PV generation supports major load demand and battery charging
500	1300	700	2000	Moderate PV contribution with partial grid support
10	700	1300	2000	Low PV generation causes higher grid power contribution
500	1300	700	2000	PV output recovers and inverter contribution increases
1000	1500	500	2000	Maximum inverter power restored with reduced grid dependency

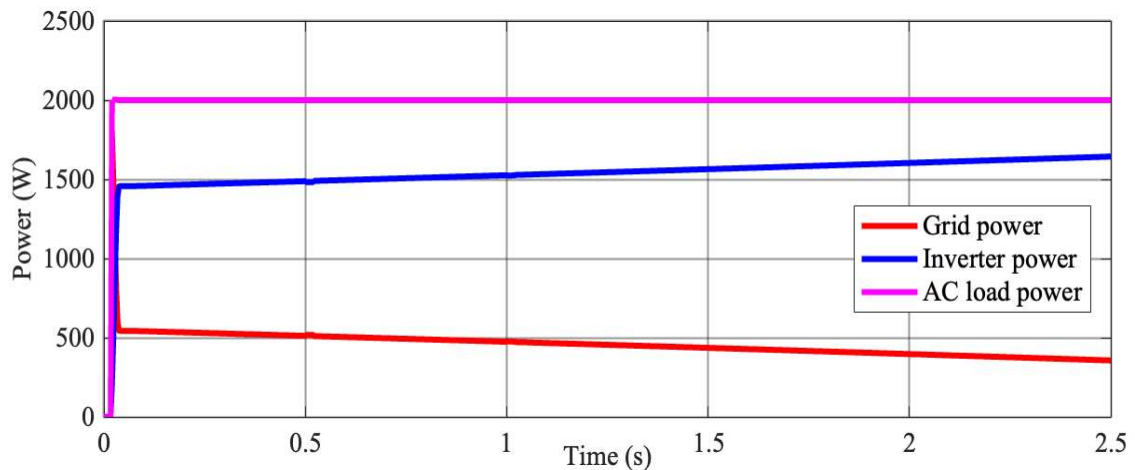


Fig. 4.10 Grid power, Inverter power and AC load power

4.3 DISCUSSION

The simulation results show that the suggested PV–BESS grid-connected system operates efficiently and in unison under a variety of load and environmental circumstances. According to the investigation, every main subsystem—including the grid-side inverter, DC-link controller, boost converter, PV array, and BESS operates steadily and dependably. Under varying solar irradiation circumstances, the implemented MPPT controller effectively keeps the PV system operating close to the MPP, guaranteeing effective use of the available solar energy with few oscillations and steady converter performance.

By working in controlled charging and discharging modes in accordance with system power requirements, the BESS efficiently adjusts for variations in PV output. The battery's State of Charge (SOC) stays within safe operating bounds, demonstrating effective battery energy management and dependable system operation. Furthermore, the DC-link voltage controller ensures smooth inverter operation and balanced power flow throughout the system by maintaining a steady DC bus voltage in spite of fluctuations in PV generation and load demand. Stable power transfer and dependable synchronization with the utility grid are provided by the grid-side inverter, PLL synchronization, and dq-axis control. All things considered, the coordinated control techniques successfully meet changing power demand requirements while ensuring a steady and continuous power supply to the linked load.

CHAPTER 5

CONCLUSION AND FUTURE SCOPE

5.1 INTRODUCTION

The modeling, control, and performance analysis of a three-phase grid-connected PV system supported by a BESS were given in this dissertation. The suggested system was created to solve the problems brought on by solar energy's sporadic nature and to provide steady and dependable power delivery to the connected load under a range of operating circumstances. The MATLAB/Simulink environment was used to model and analyze the entire system, including the PV array, DC–DC boost converter, BESS, bidirectional converter, DC-link, grid-connected inverter, and control techniques.

Under various irradiance conditions, the MPPT technique was effectively used to harvest the maximum power available from the PV array. Through regulated charging and discharging operations, the BESS successfully managed energy balance, adjusting for variations in PV generation and ensuring a steady power supply to the load. While the grid-side inverter with dq-axis control and PLL synchronization guaranteed solid grid interfacing and dependable power transfer, the DC-link voltage controller maintained steady DC bus voltage.

The outcomes of the simulation showed that the suggested PV-BESS integrated system functions well under environmental circumstances. System stability, smooth power flow, dependable inverter operation, and overall energy management were all improved by the coordinated control measures. The PV system's ability to meet fluctuating load demands and sustain uninterrupted power delivery during variations in solar generation was greatly enhanced by the integrated battery storage technology. All things considered, the suggested PV–BESS grid-connected system offers an effective, dependable, and

sustainable option for power applications based on renewable energy. Future real-time implementation, sophisticated energy management techniques, and additional research in grid-integrated renewable energy systems can all benefit from the developed model and control framework.

5.2 KEY CONTRIBUTIONS AND CONCLUSION

This dissertation uses the MATLAB/Simulink environment to give a thorough modeling and control framework for a three-phase grid-connected PV system backed by a BESS. To optimize solar power extraction under changing temperature and irradiance circumstances, an efficient MPPT management mechanism has been put into place. To provide a steady, continuous power supply to the linked load, a bidirectional battery energy management system has also been implemented for controlled charging and discharging.

For dependable grid integration and steady power transmission, the task also involves implementing sophisticated control techniques including DC-link voltage regulation, dq-axis inverter control, and PLL synchronization. Additionally, the effectiveness and dependability of the suggested PV–BESS integrated system have been demonstrated by evaluating the overall system performance under various operating conditions, such as

Developed a comprehensive modeling framework utilizing the MATLAB/Simulink environment for a three-phase grid-connected PV system supported by a BESS.

5.3 LIMITATIONS

5.3.1 Limited to Simulation Validation

Only simulation studies in the MATLAB/Simulink environment are used to validate the suggested PV–BESS integrated system; real-time hardware implementation is not included in this work.

5.3.2 Simplified Battery Modelling

Long-term deterioration effects and detailed thermal behavior are not included in the battery model utilized in this work, which could affect actual battery performance during protracted operation.

5.3.3 Limited Grid Disturbance Analysis

The performance under large-scale grid disruptions or fault circumstances has not been thoroughly examined, and the study is restricted to a particular system architecture and control method.

5.4 FUTURE SCOPE

In the event of low solar irradiation, unfavorable weather, or low battery charge levels, the suggested PV–BESS integrated system may be further improved to enable intelligent grid-support operation. To provide consistent and dependable power supply under such operating circumstances, electricity may be sent straight from the utility grid to the linked load. This strategy may assist sustain steady functioning in a variety of environmental situations and increase overall system dependability. For effective coordination of the utility grid, Battery Energy Storage System (BESS), and photovoltaic (PV) system, advanced energy management and intelligent control approaches may be created. Effective power sharing, better energy use, and a steady power supply under varying load demand situations may all be made possible by these management systems. Future research may also concentrate on enhancing the overall performance of the grid-connected system by using sophisticated inverter management strategies and filtering techniques to lessen harmonics, voltage fluctuations, and other disturbances.

Additionally, real-time hardware implementation and experimental validation of the suggested PV–BESS integrated system under realistic operating circumstances may be included in future study. System dependability, operational effectiveness, controller performance, and dynamic responsiveness under real-world environmental and load fluctuations may all be assessed with the use of hardware-based testing. This would strengthen the basis for the widespread implementation of grid-connected power systems powered by renewable energy.

APPENDICES

Appendix 1 : MATLAB/Simulink Code for MPPT Control

```
% author : Saad MOTAHHIR
% f= 10000hz (G)
function D = INC(V, I)

Dinit = 0.42; %Initial value for D output
Dmax = 0.95; %Maximum value for D
Dmin = 0.01; %Minimum value for D
deltaD = 0.000005; %Increment value used to increase/decrease the duty cycle
D

persistent Vold Pold Dold M Iold;

dataType = 'double';

if isempty(Vold)
    Vold=0;
    Pold=0;
    Iold=0;
    Dold=Dinit;
    M=1;
end
P= V*I;
dV= V - Vold;
dP= P - Pold;
dI= I - Iold;
M=1;

if M < 0.005
    D=Dold;
else
    if dV == 0
        if dI == 0
            D=Dold;
        elseif dI>0
            D=Dold - (M*deltaD);
        else
            D=Dold + (M*deltaD);
        end
    else
        if dI/dV == -I/V
            D=Dold;
        elseif dI/dV>-I/V
            D=Dold - (M*deltaD);
        else
            D=Dold + (M*deltaD);
        end
    end
end
end
```

```
if D >= Dmax | D <= Dmin  
    D=Dold;  
end
```

```
Dold=D;  
Vold=V;  
Pold=P;  
Iold=I;
```

Appendix 2 : Design Calculation of Inductance, Capacitance, and Resistance of Boost Converter

```
Vin=460.5;  
fs=10e3;  
Vout=700;  
Ioutmax=(250*15*2)/Vout;  
delIL=0.1*Ioutmax*(Vout/Vin);  
delvout=0.1*Vout;  
L=(Vin*(Vout-Vin))/(delIL*fs*Vout)  
C=(Ioutmax*(1-(Vin/Vout)))/(fs*delvout)  
R=Vout/Ioutmax
```

REFERENCES

- [1] Purohit, “Techno-Economics of Grid Connected Battery Energy Storage Systems for Renewable Energy Integration in India,” *Global Energy Interconnection*, vol. 9, no. 1, pp. 1–12, 2026, doi: 10.1016/j.gloi.2026.01.011.
- [2] H. Patel and V. Agarwal, “MATLAB-based modeling to study the effects of partial shading on PV array characteristics,” *IEEE Transactions on Energy Conversion*, vol. 23, no. 1, pp. 302–310, Mar. 2008.
- [3] J. A. Duffie and W. A. Beckman, *Solar Engineering of Thermal Processes*, 4th ed., Wiley, 2013.
- [4] R. Teodorescu, M. Liserre, and P. Rodríguez, *Grid Converters for Photovoltaic and Wind Power Systems*, Wiley-IEEE Press, 2011.
- [5] A. Khaligh and Z. Li, “Battery, ultracapacitor, fuel cell, and hybrid energy storage systems for electric, hybrid electric, fuel cell, and plug-in hybrid electric vehicles,” *IEEE Transactions on Vehicular Technology*, vol. 59, no. 6, pp. 2806–2814, Jul. 2010.
- [6] D. A. Rodrigues et al., “Hybrid energy storage control strategy for PV applications,” *IEEE Transactions on Sustainable Energy*, vol. 11, no. 2, pp. 982–991, Apr. 2020.
- [7] N. Femia, G. Petrone, G. Spagnuolo, and M. Vitelli, “Optimization of perturb and observe maximum power point tracking method,” *IEEE Transactions on Power Electronics*, vol. 20, no. 4, pp. 963–973, Jul. 2005.
- [8] H. Akagi, E. H. Watanabe, and M. Aredes, *Instantaneous Power Theory and Applications to Power Conditioning*, Wiley-IEEE Press, 2007.
- [9] International Energy Agency, *Net Zero by 2050: A Roadmap for the Global Energy Sector*, IEA, Paris, 2021.
- [10] H. A. Sher, K. E. Addoweesh, and A. H. Abdel Ghaffar, “A survey of PV system growth and performance trends,” *IEEE Access*, vol. 6, pp. 13622–13635, 2018.
- [11] H. Patel and V. Agarwal, “MATLAB-based modeling to study the effects of partial shading on PV array characteristics,” *IEEE Transactions on Energy Conversion*, vol. 23, no. 1, pp. 302–310, Mar. 2008.

- [12] D. A. Rodrigues, C. C. Gomes, and J. P. F. Trovão, "A hybrid energy storage system for smoothing photovoltaic power fluctuations," *IEEE Transactions on Sustainable Energy*, vol. 11, no. 2, pp. 982–991, Apr. 2020.
- [13] T. Kerdphol, Y. Qudaih, and Y. Mitani, "Battery energy storage system for improving stability and reliability of microgrid," *IEEE Transactions on Industry Applications*, vol. 54, no. 1, pp. 1–9, Jan. 2018.
- [14] H. Patel and V. Agarwal, "MATLAB-based modeling to study the effects of partial shading on PV array characteristics," *IEEE Transactions on Energy Conversion*, vol. 23, no. 1, pp. 302–310, Mar. 2008.
- [15] M. A. Hannan, M. S. Hossain Lipu, A. Hussain, and A. Mohamed, "A review of lithium-ion battery state of charge estimation and management systems in electric vehicle applications," *IEEE Access*, vol. 6, pp. 19362–19378, 2018.
- [16] R. Teodorescu, M. Liserre, and P. Rodríguez, *Grid Converters for Photovoltaic and Wind Power Systems*, Wiley-IEEE Press, 2011.
- [17] J. M. Guerrero, P. C. Loh, T. Lee, and M. Chandorkar, "Advanced control architectures for intelligent microgrids—Part I: Decentralized and hierarchical control," *IEEE Transactions on Industrial Electronics*, vol. 60, no. 4, pp. 1254–1262, Apr. 2013.
- [18] R. Teodorescu, M. Liserre, and P. Rodriguez, *Grid Converters for Photovoltaic and Wind Power Systems*, Wiley-IEEE Press, 2011.
- [19] N. Femia, G. Petrone, G. Spagnuolo, and M. Vitelli, "Optimization of perturb and observe maximum power point tracking method," *IEEE Transactions on Power Electronics*, vol. 20, no. 4, pp. 963–973, Jul. 2005.
- [20] U. Madawala and D. J. Thrimawithana, "A bidirectional grid interface for electric vehicles with V2G capability," *IEEE Transactions on Industrial Electronics*, vol. 58, no. 10, pp. 4789–4796, Oct. 2011.
- [21] S. Dasgupta, S. N. Mohan, S. K. Sahoo, and S. K. Panda, "Application of Four-Switch-Based Three-Phase Grid-Connected Inverter to Connect Renewable Energy Source to a Generalized Unbalanced Microgrid System," *IEEE Transactions on Industrial Electronics*, vol. 60, no. 3, pp. 1204–1215, Mar. 2013.
- [22] Y. W. Li and C. N. Kao, "An Accurate Power Control Strategy for Power-Electronics-Interfaced Distributed Generation Units Operating in a Low-Voltage Multibus Microgrid," *IEEE Transactions on Power Electronics*, vol. 24, no. 12, pp. 2977–2988, Dec. 2009.

- [23] W. Tushar, C. Yuen, T. Saha, and H. V. Poor, "Peer-to-Peer Energy Systems for Connected Communities: A Review of Recent Advances and Emerging Challenges," *Applied Energy*, vol. 282, pp. 116–131, 2021.
- [24] T. Wang, Y. Liu, and X. Zhang, "Research on Grid-Connected Control Strategy of Photovoltaic and Energy Storage Integrated System," *Energies*, vol. 16, no. 24, pp. 1–19, 2023.
- [25] A. Jain and S. Bhullar, "Design and Performance Analysis of Solar PV-Battery Energy Storage System Integration with Three-Phase Grid," *Journal of Power Sources*, vol. 640, pp. 236486, 2025.
- [26] P. K. Bera, S. R. Pani, C. Isik, and R. C. Bansal, "A Hybrid Intelligent System for Protection of Transmission Lines Connected to PV Farms," *IEEE Access*, vol. 12, pp. 1–15, 2024.
- [27] . M. S. Al Khdhairi, "Large-Scale Battery Energy Storage System Integration to Improve Grid Stability," *Journal of Renewable Energy and Environment*, vol. 12, no. 2, pp. 45–58, 2025.
- [28] Y. Gu and T. C. Green, "Power System Stability with High Penetration of Inverter-Based Resources," *Proceedings of the IEEE*, vol. 110, no. 11, pp. 1–15, 2022.
- [29] F. Blaabjerg, Y. Yang, D. Yang, and X. Wang, "Distributed Power-Generation Systems and Protection," *Proceedings of the IEEE*, vol. 105, no. 7, pp. 1311–1331, Jul. 2017.
- [30] H. Cha, T. K. Vu, and J. E. Kim, "Design and Control of Proportional–Resonant Controller Based Photovoltaic Power Conditioning System," *Energies*, vol. 7, no. 3, pp. 1848–1864, 2014.
- [31] M. Castilla, J. Miret, J. Matas, L. G. de Vicuña, and J. M. Guerrero, "Control Design Guidelines for Single-Phase Grid-Connected Photovoltaic Inverters with Damped Resonant Harmonic Compensators," *IEEE Transactions on Industrial Electronics*, vol. 56, no. 11, pp. 4492–4501, Nov. 2009.
- [32] J. Hu, J. Zhu, and D. G. Dorrell, "Model Predictive Control of Grid-Connected Inverters for PV Systems," *Electric Power Systems Research*, vol. 189, pp. 1–10, Dec. 2020.

PUBLICATION

VINEET GAUTAM

2K24/PSY/04

M.tech (Power System), Electrical Engineering, Delhi Technological University

Email: vineetgautam_24psy04@dtu.ac.in

1. Conference Paper

Title: Battery Energy Storage Supported Three-Phase Grid-Connected PV System

Authors: VINEET GAUTAM, RACHNA GARG, KULDEEP SINGH

STATUS:

DOI: <https://doi.org/10.1109/IC3ECSBHI67834.2026.11468949>

IEEE CONFERENCE: 2026 2ND International Conference on Cognitive Computing in Engineering, Communication, Sciences and Biomedical Health Informatives (IC3ECSBHI)